

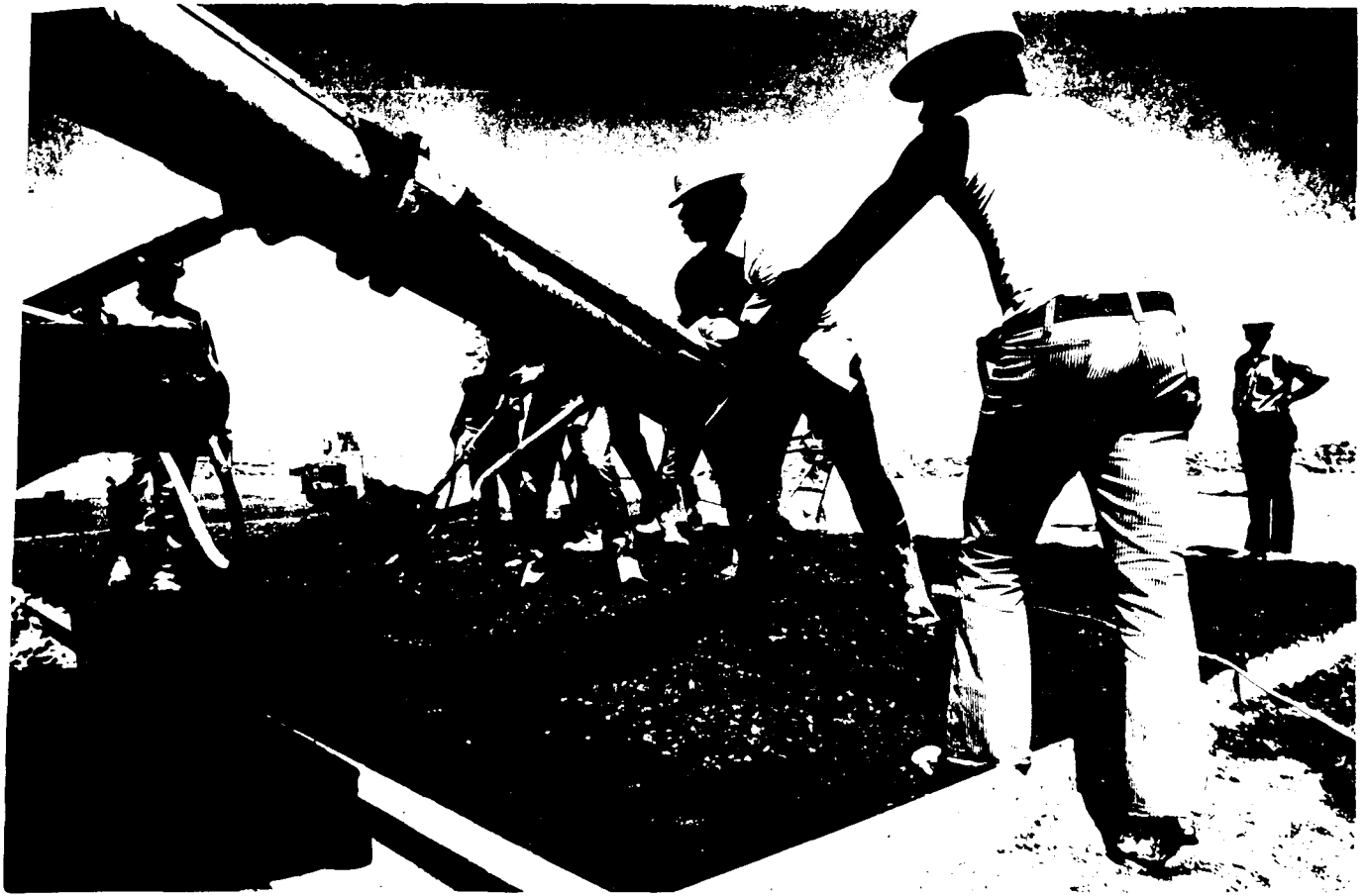
**ACCELERATED TRIALS OF  
GLASS FIBER REINFORCED RIGID PAVEMENTS**

by: Ernest L. Buckley, P.E., Ph.D.

April 12, 1974

Civil Engineering Research

Published by  
The Construction Research Center  
College of Engineering  
University of Texas at Arlington  
Arlington, Texas 76019



Frontispiece: THE FIRST FIELD PLACEMENT OF GLASS FIBER REINFORCED CONCRETE FROM TRANSIT MIXER

#### ACKNOWLEDGEMENTS

The author wishes to acknowledge the contributing efforts of all those whose assistance and support made this work possible.

These include:

- (1) Mr. Ray Masters, Gifford-Hill Company
- (2) Mr. Ken Earhart, Mr. Robert Peyton, and Mr. Jimmy Munn of Gifford-Hill Cement Company, Midlothian Division.
- (3) Mr. Jimmy D. George and Mr. W. E. (Baldy) Hodge of J. L. Bertram Construction and Engineering Co.
- (4) Mr. William Pansius and Mr. Henry Marsh of Owens-Corning Fiberglas Technical Center.
- (5) Mr. S. L. Anderson of Cush-Crete Inc.
- (6) Mr. Mike Shiflett, Mr. John McRoberts, Mr. H. S. (Scott) Coltar, and Mr. Robert Hill, all graduate students at the University of Texas at Arlington.

ACCELERATED TRIALS OF  
GLASS FIBER REINFORCED RIGID PAVEMENTS

Table of Contents

Section 1	:	INTRODUCTION	Page 1
Section 2	:	BACKGROUND	8
Section 3	:	CONSTRUCTION	16
Section 4	:	DEFLECTION MEASUREMENTS	25
Section 5	:	OBSERVED PERFORMANCE	33
Section 6	:	PERFORMANCE EVALUATION	40
6.1	:	Serviceability Performance Analysis	41
6.2	:	Flexural Stress Analysis	49
6.3	:	Conclusions	60

## SECTION 1

### INTRODUCTION

For over a decade, research has been done to develop the concept of fibrous reinforcement of Portland Cement concrete. Short, randomly oriented fibers, evenly distributed through the concrete, enhance flexural strength, ductility and fracture toughness. At the Civil Engineering Department, College of Engineering, of the University of Texas at Arlington, work was begun in 1970 which lead to the conclusion that glass fiber, because of its relatively low elastic modulus, is the best of the fibrous materials currently available for use as a concrete reinforcement.

The theoretical development, along with a comprehensive experimental program, indicates that glass fiber reinforcement applications are numerous. Its use as a substitute for the steel bars that are the principal tension reinforcement in beams and frames is not advocated. The most promising applications are those where relatively thin sections of concrete must accomodate complex loads and stress combinations. Rigid pavements are a classic example of this category of concrete structure. The performance of a concrete pavement slab involves complex interactions between the pavement and a varied array of loads and between the pavement and its supporting

sub-grade. Steel reinforcement is normally placed at mid-depth where it resists thermal and shrinkage stresses, but where it is relatively ineffective in resisting flexural stresses.

Because of the theoretically favourable effects of providing randomly oriented, short, glass fiber reinforcement for rigid pavement, the test project, that is the subject of this report, was planned and executed. The objectives of the project were as follows:

- 1) To gain experience and to extend techniques developed in the laboratory to the field mixing, placement and finishing of glass fiber reinforced concrete in quantity.
- 2) To compare the performance of glass reinforced rigid pavements of varying depths to the municipal standard street pavement in common use.
- 3) To evaluate all data and, therefore, to provide recommendations and criteria for design of glass fiber reinforced pavements and slab-on-ground foundations and flat-work.

Carried on in parallel with the service test reported here were comparative tests made of the concept of using recycled, granulated, rubber tire material as a resilient interface layer for rigid pavements. The results of those tests will be made a separate report that will be published at a later date.

The test plan, that was developed, provided for the construction of five test slabs 16' x 20' as shown by Figure 1. The test site, in the quarry of Gifford-Hill Cement Company Midlothian Division, permitted

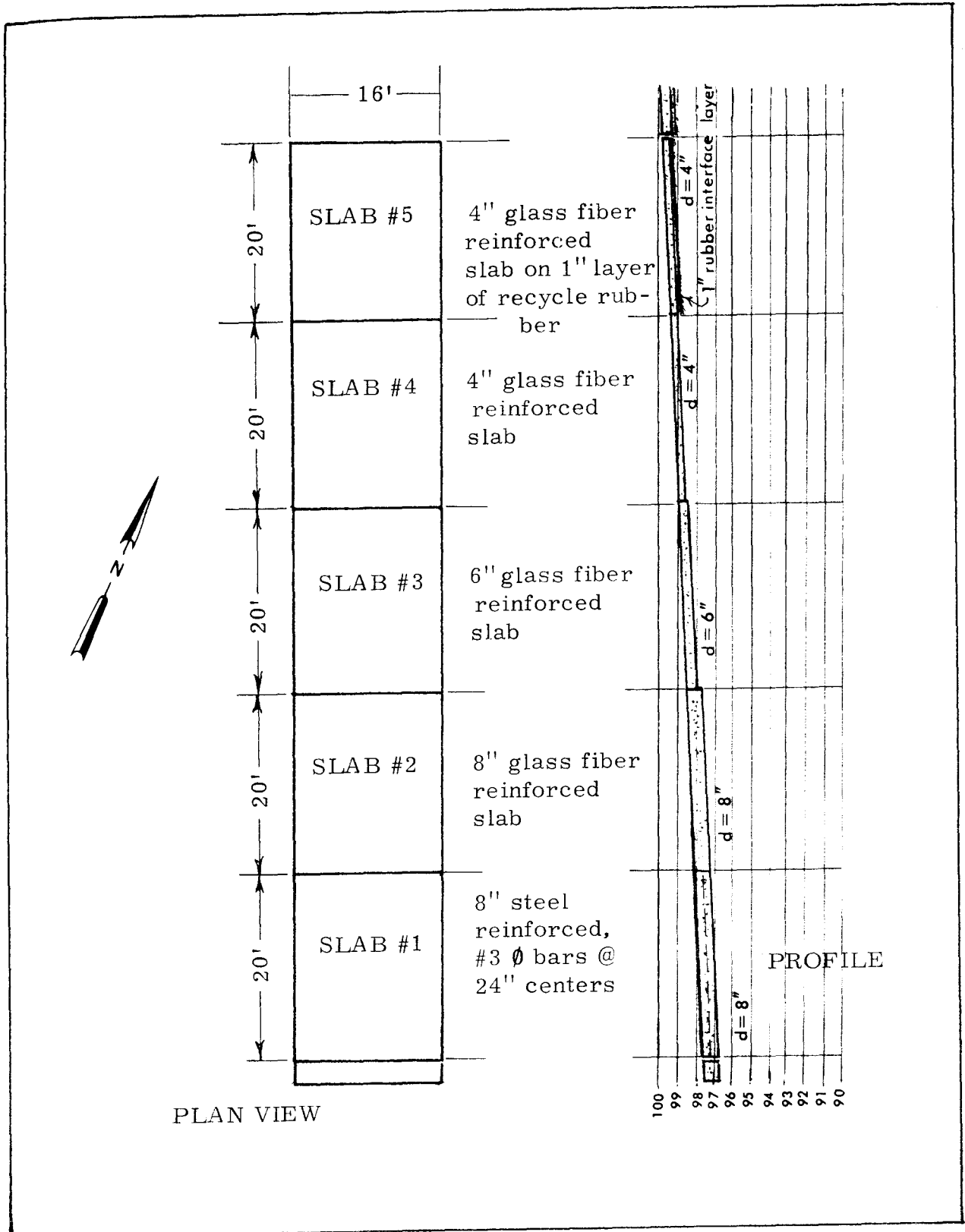


Figure 1: TEST SITE LAYOUT

the use of large, heavy Euclid rock haulers as test loads that will produce accelerated test results.

Glass fibers were furnished by Owens-Corning Fiberglas Technical Center, Granville, Ohio. Concrete was furnished by Gifford-Hill Company, Inc., Dallas, Texas. Construction labor and equipment was provided by J. L. Bertram Construction and Engineering Company. The test slabs were poured and cured, subjected to static and dynamic load deflection tests, and then placed under repetitive loading to failure.

For evaluation of performance, the basic design criteria established by the American Association of State Highway Officials (AASHO) and that criteria developed by the Portland Cement Association (PCA) was used. The PCA method provides for the design of the pavement thickness that avoids the evidence of initial distress, "first crack." The AASHO method is primarily concerned with the capacity of a pavement to provide adequate ride quality while subject to repetitive loading.

The results of the tests, evaluated in terms of both the PCA method and the AASHO method, are summarized as follows:

- 1) The 6-inch pavement of Slab #3 and the 8-inch pavement of Slab #2, both reinforced with glass fibers showed better performance with respect to first crack than did

the 8-inch conventional pavement with steel reinforcement.

- 2) Similarly, Slab #3 performed better, in terms of Serviceability Index, than the control Slab #1 up to about 400,000 equivalent 18 kip single axle load repetitions and at a Serviceability Index  $p = 3.0$ . Slab #2, 8-inch glass reinforced concrete, continued throughout the test to perform better than the conventional steel reinforced 8-inch Slab #1. At the end of the test, Slab #1 had deteriorated to  $p=1.8$ , while Slab #2 had a Serviceability Index  $p=2.1$ . See Figure 2. The superiority of performance is significant since the basic strength of the concrete matrix of Slabs #2 and #3 was 43% and 77%, respectively, of the compressive strength of the control Slab #1.
- 3) Slab #4 showed early distress and had reached a terminal condition at 124,000 equivalent 18 kip single axle load repetitions.
- 4) Slab #5, incorporating a granulated rubber interface layer between the pavement and its sub-grade, failed immediately under test loads.

It should be noted that this service test project involved the largest single pour of glass fiber reinforced concrete made up to this time. It was the first time that glass fiber reinforced concrete, in practical proportions for field use, was poured from a transit mixer. The glass fibers, added at the job site and mixed for up to 5 minutes at maximum drum speed, were thoroughly distributed through the mix.

In future work of this kind, a mix with an increased amount of cement is recommended. The glass fibers could probably be chopped and added at the transit mixer, using an electric or pneumatic chopper, with less manual effort. For this test the fibers were pre-chopped and



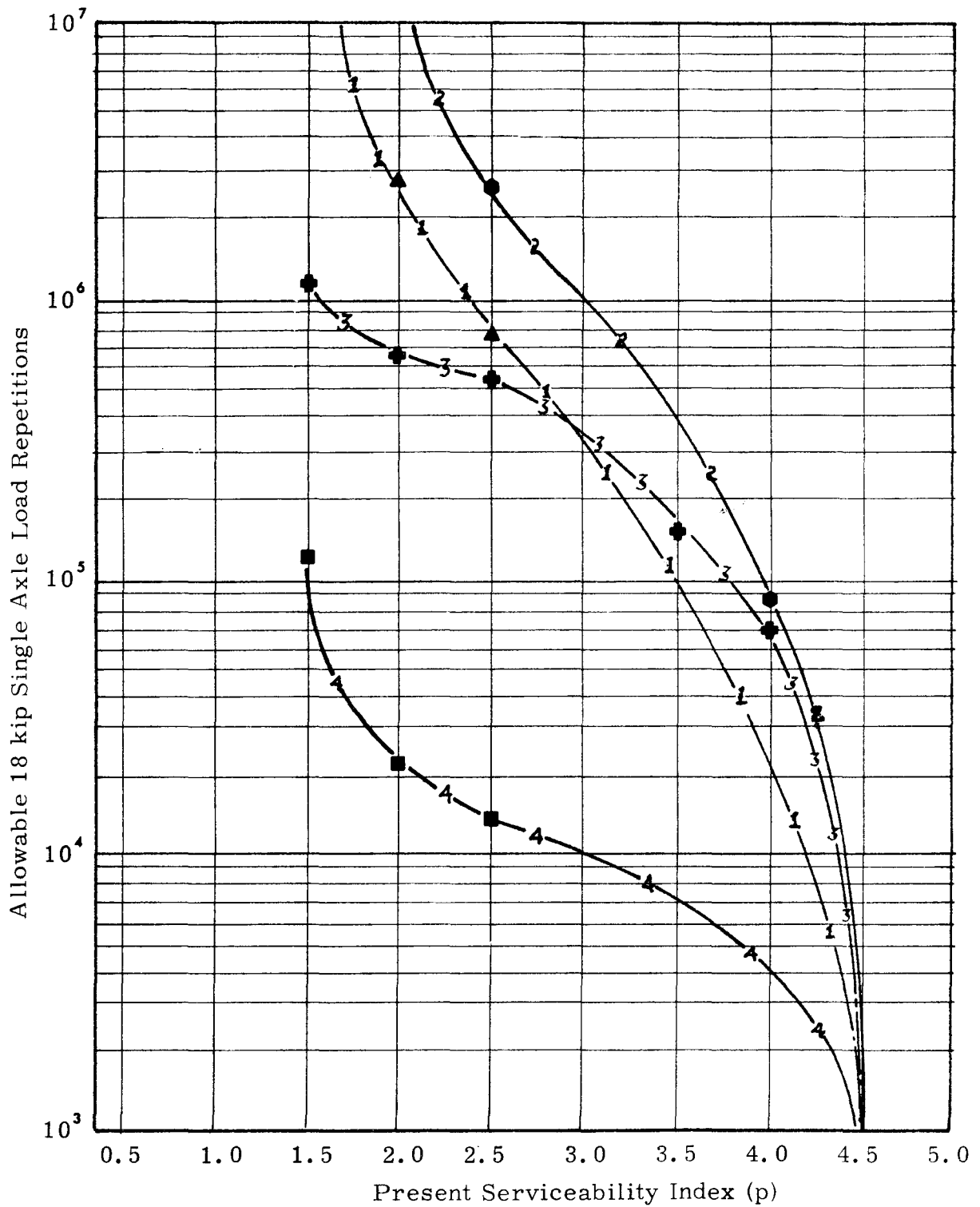


Figure 2: SUMMARY OF TEST SLAB PERFORMANCE  
(see discussion in Section 6 and Table 6-4)

dumped into the mixer by hand, directly from the 50 pound cardboard shipping containers.

The low-slump characteristic of the glass fiber and concrete mix requires vibration during placement. An adequate number of high-energy, high frequency vibrators should be available for any future work.

All objectives of the test project were met and the feasibility of glass fiber reinforced concrete pavements, with improved performance has been shown. Further testing can serve to optimize concrete batch proportions and placement techniques.

SECTION 2  
BACKGROUND

Investigations were begun early in 1970 at the University of Texas at Arlington of the physical characteristics of various kinds of fibrous materials that might be used as reinforcements for Portland Cement Concrete Mortar. Laboratory tests were made to determine the properties of mortar and concrete matrices reinforced with boron, graphite and glass fibers. Data was compiled and evaluated for the purpose of optimizing mix proportions and for determining compressive strength, tensile strength, flexural strength, ductility and fracture toughness. In these tests it was found that glass fibers perform best, as compared to boron or graphite. The results also indicate that glass fibers perform better as a concrete reinforcement than do steel fibers.

Small, short, steel wire fibers have been used with considerable success for a wide variety of test specimens and in full-scale service tests of pavements, floor slabs and structural members. Difficulties have been experienced in handling and dispersing the steel fibers. They tend to form "balls" of tightly interlocked fibers and they are hazardous to workmen during mixing and placement operations. Never-the-less, the promising potential of the concept,

substituting fiber reinforcement for conventional steel reinforcing bars, has been thoroughly demonstrated by those who have investigated steel fiber reinforced concrete.

All of the materials tested at the Construction Research Center at UTA are characterized by low weight and high tensile strength. Boron fibers have an elastic modulus that is almost twice that of steel. The elasticity of the graphite fibers used is comparable to steel, although formulations with a much higher modulus can be produced. The glass fibers used are a new alkali resistant material, produced by Owens-Corning Fiberglas, with an elastic modulus of about one-third that of steel. It was believed, at the outset that a high modulus of elasticity would have positive influence on the performance of a fiber reinforced mortar or concrete. Subsequent development of theory, verified by testing, shows that the reverse is true. The glass fibers appear to be a superior reinforcement material.

Theory, relating to the mechanism through which fibers improve the performance of a brittle matrix, is based upon the Griffith model of brittle fracture. Using an energy balance approach, the critical modulus of rupture for a fiber reinforced mortar or concrete can be predicted by the equation:

$$f_r = \sqrt{\frac{2TE_c}{(1-\mu^2)\pi c} + \frac{(u\lambda)^2 Lp}{928(1-\mu^2)nc}}$$

where  $T$  is the surface energy absorbed in the formation of cracks per unit of crack area,

$E_c$  is the elastic modulus of the composite material determined by calculations based upon the "theory of mixtures".

$\mu$  is Poissons ratio for the concrete matrix.

$c$  is the half-crack length of the critical crack or flaw

$u$  is the unit bond stress

$\lambda$  is the aspect ratio or length of the fiber over its effective diameter

$L$  is the length of the fiber

$p$  is the fiber content expressed as a percent of total volume

$n$  is the modular ratio, the Young's modulus of the reinforcement ( $E_r$ ) over the modulus of the concrete or mortar matrix ( $E_m$ ).

Typical properties of concrete, that may be used in calculations employing the equation, are shown in Table 2-1.

The theoretical equation has been evaluated by extensive tests involving boron, graphite and glass fiber reinforcements in concrete and mortar. Comparisons have also been made to the results reported by others who have used short, steel wire fibers for reinforcement. The validity of the equation has been established within the following limits:

- 1) The aspect ratio is limited to values of about 100 for laterally stiff fibers. For glass fibers, aspect ratios

up to about 135 (L = 1.5 inches) have been used, and the upper limit may be assumed to be about 2 inches.

- 2) The volume percentage  $p$  is limited by the adsorption characteristics displayed by all fibers which affects workability. Values of  $p$  of up to 4 or 5 percent have been used in the laboratory. Fiber content of from 1.5 to 2.0 percent by volume appears to be the practical limit for field applications.
- 3) Developable bond stress in steel wire fibers may be about 400 psi. Values of  $u$  for glass fibers have been approximated at about 200 psi by indirect methods. Work is continuing to change surface chemistry and increase the bond.
- 4) The modular ratio in the denominator indicates that low modulus materials, like glass, are superior to high modulus fibers. The lower limiting value would be when  $E_r = E_m$  or  $n = 1$ .

The test program showed boron to have the same disadvantages as steel wire fibers with respect to the "balling" problem and with respect to the hazards in handling the stiff, needle-like fibers. The experience of handling and placing boron reinforced concrete is hazardous because of the small diameter, stiff fibers are like needles. Exposed concrete, reinforced with steel wire or boron fibers, would be a continuing hazard. Boron is, in any case, too expensive to be a practical reinforcement.

Graphite fiber appears to have potential but cannot be practically used in the form of yarn-like bundles of 10,000 filaments that

TABLE 2-1  
TYPICAL PROPERTIES OF CONCRETE

Ultimate Compressive Strength $f'_c$ (psi)	Modulus of Elasticity E (psi x $10^6$ )	Poissons Ratio $\mu$	Surface Tension T (in lbs/in <sup>2</sup> )	Critical Half-crack Length c (inches)
2000	2.58	0.20	0.015	0.637
4000	3.64	0.16	0.035	0.641
6000	4.46	0.12	0.042	0.598
8000	5.15	0.11	0.050	0.538

were used. Dispersal of the chopped strands was inhibited by cohesion of the filaments in the presence of water. Individual filaments appear to bond effectively, but only the exterior filaments at the periphery of the bundle are "wetted" by the cement paste. The interior filaments are unbonded and fail by pull-out. To be useful, strands of these tiny filaments will require some high-strength coating or sizing so that they can be dispersed and effectively bonded to the matrix of mortar or concrete.

Glass fibers, of alkali-resistant formulations, appear to be

a practical reinforcement material with the desired properties. Like other fibers, surface adsorption of mixing water produces a stiff, unworkable mix at high concentrations of the fibers. Best results are obtained at fiber content of 1.5 to 2.0 percent by volume with heavy vibration used for compaction during placement. The fibers disperse with relative ease. There are no hazards in handling nor in the finished product.

Using the theoretical equation that was described above and the values for the properties of concrete shown in Table 2-1, the predicted performance of glass reinforced concrete is shown as a function of volume content in percent by Figure 3. Empirical data points, for a concrete matrix of compressive strength of 5000 psi, are also plotted and show reasonably close correlation to theoretical values for a developed bond stress of about 200 psi.

Potential practical application of glass fiber reinforced concrete are numerous. Thin sections, where cover requirements result in disadvantageous placement of steel reinforcing bars, are most attractive. Slab-on-grade foundations for buildings, pre-cast architectural panels, and concrete products such as pipe, are examples. Streets and highway pavements are considered to be an especially promising application.



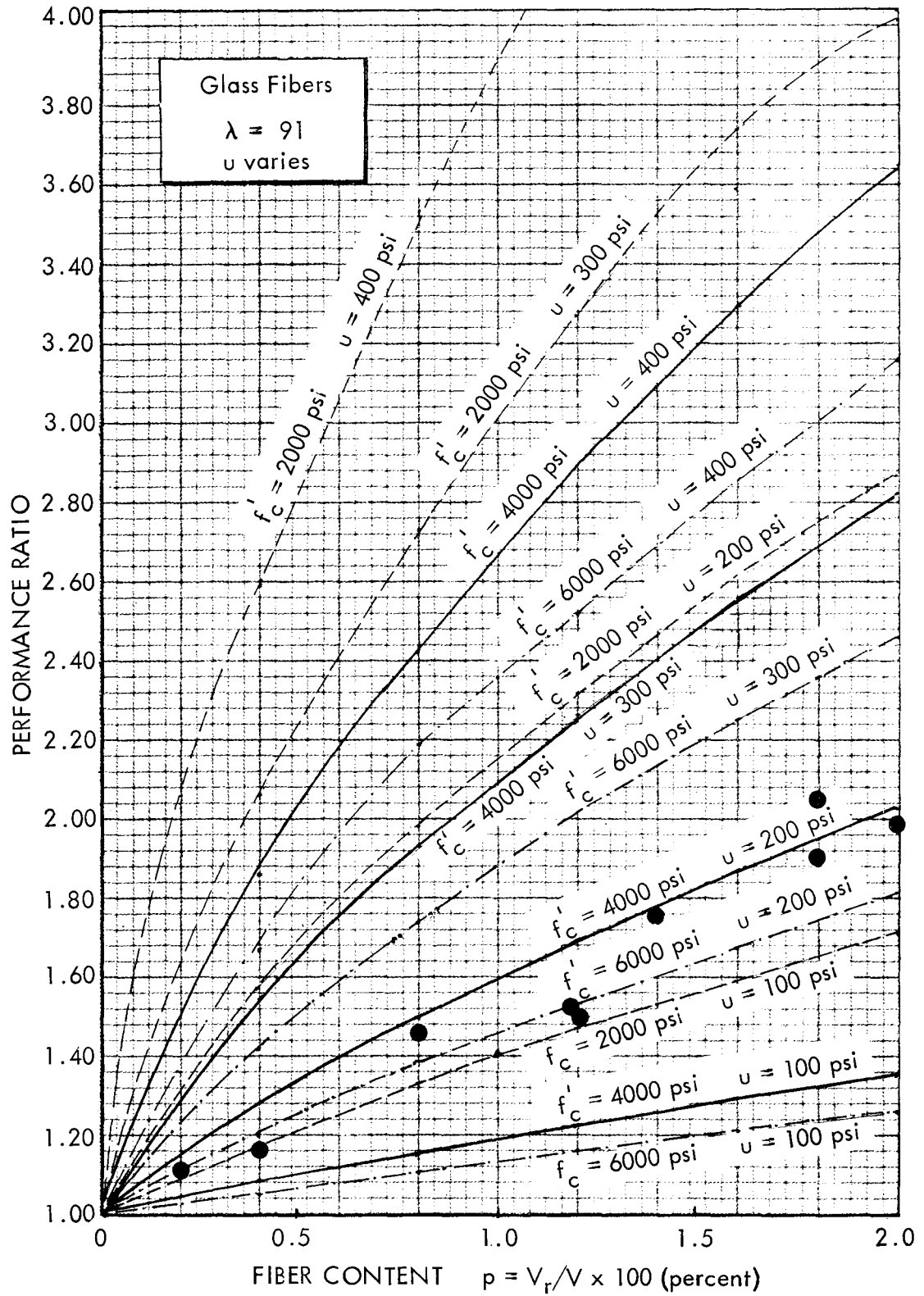


Figure 3: THEORETICAL PERFORMANCE OF GLASS FIBER REINFORCED CONCRETE

Municipal standards for rigid concrete pavements vary; however, the standard employed by the City of Dallas are fairly typical. Specifications call for concrete with 5 sacks of cement per cubic yard, 28-day compressive strength  $f'_c = 3000$  psi,  $1\frac{1}{2}$ " maximum aggregate size, and gradation in accordance with ASTM C-33. Reinforcement required is #3  $\emptyset$  bars, at 24-inches on center, both ways, placed at the middle depth of an 8-inch slab. With this placement, there is no reinforcement for flexural stresses. Cracking is a common occurrence and is often the first step in failure - admission of moisture to the sub-grade, pumping, loss of sub-grade support, and complete loss of serviceability.

Fibrous reinforcement places randomly oriented fibers, uniformly distributed, throughout the concrete matrix. Flexural strength can be substantially increased since reinforcement is provided at the extremities of the section. Improvement in ductility and fracture toughness can also be of benefit in avoiding or postponing evidence of initial distress under repetitive vehicular loads.

The apparent advantages that could be gained through the use of glass fiber reinforcement led to the planning, preparation and execution of the service tests described in this report.

SECTION 3  
CONSTRUCTION

To investigate the problems of placement and the performance of glass fiber reinforced pavements, the full-scale service test described in this report was planned and executed. The objective of the test was to demonstrate the feasibility of using glass fibers for the principal reinforcement of pavement slabs.

The selected test site is on the haul road on the floor of the quarry operated by the Gifford-Hill Cement Company, Midlothian Division. The modulus of sub-grade reaction "k" was conservatively estimated to be 400 kips per square inch per inch. The test loads would be provided by fully loaded Euclid rock-hauling vehicles of a gross vehicle weight of 128,300 lbs.

The configuration of the test track was as shown by Figure 1, Section 1, herein. At each end of the 16 ft. wide test lane, an unreinforced transition slab, 3 ft. long, was constructed to keep impact loads of approach and departure off of the test slabs. With reference to Figure 1, the 20 ft. long test slabs are identified as follows.

Slab No. 1: An 8-inch conventionally reinforced concrete pavement slab, meeting municipal standards, reinforced by #3 bars at 24-inches on center both ways, served as the control slab. The performance of all the other slab configuration was then compared to the standard configuration.

Slab No. 2: An 8-inch slab, with glass fiber reinforcement, at about 1% by volume, was built to show the relative performance of fibers as a substitute reinforcement.

Slab No. 3: A 6-inch glass fiber reinforced slab, with fiber volume of about 1%, was placed to determine the effect of substituting fibers for conventional reinforcement and reducing the depth of the section.

Slab No. 4: A 4-inch slab, reinforced with about 1% glass fibers by volume, was constructed to demonstrate the effects of substituting fibers for steel and further reducing the cross section depth.

Slab No. 5: A 4-inch slab was built with a resilient interface layer, between the slab and the sub-grade, made of synthetic recycled rubber material 1-inch thick. This was intended to show the effects of the interface layer upon the performance of a concrete pavement, reinforced with about 1.5% by volume of glass fibers and of reduced cross section.

Preparatory work was begun at the test site during the period June 18 - 25. Rough grading was accomplished by Gifford-Hill. Forms and equipment were delivered to the site by J. L. Bertram Construction and Engineering Company on June 23, were set up, and fine grading was completed on June 25.

On June 26, 1973, the rigid pavement test slabs 16 x 20 ft. were cast, by crews and equipment furnished by the Bertram Company. The objective of the project is to compare the performance of a conventional concrete pavement, built to municipal standards to the performance of glass fiber reinforced concrete pavements, pavement on

a rubber underlayment, and combinations of these two innovations. Glass fibers for the test were furnished by Owens-Corning Fiberglas. Ground rubber (recycled rubber tires), used under slab #5, was furnished by S. L. Anderson, Cush Crete Inc. Ready mix concrete and sand was furnished by Gifford-Hill Corporation.

As shown by Figure 4, steel forms 8-inches deep were used for all slabs. Well-graded sand was used to bring the sub-grade to precise elevation. Slabs #1 and #2 were placed directly upon the hard shale sub-grade. The sand provided for reduction in depth of slabs #3, #4 and #5. The sand was wetted and compacted, but probably resulted in some small reduction of the sub-grade modulus.

The concrete used for the control slab #1 was proportioned to meeting the municipal standards employed by the City of Dallas. The coarse aggregate was a crushed lime stone of 1.5" maximum size. The fine aggregate was a well-graded sand in common use in the Dallas-Fort Worth area. Cement content was 5 sacks per cubic yard, Type I Portland cement. The batch was designed for a 3-inch slump. A water reducing agent (Darex) in the amount of 3 ounces per sack was added to all concrete batches. Also a retarder (Daratard) in the amount of 8 ounces per sack was also added for all batches. Steel reinforcement

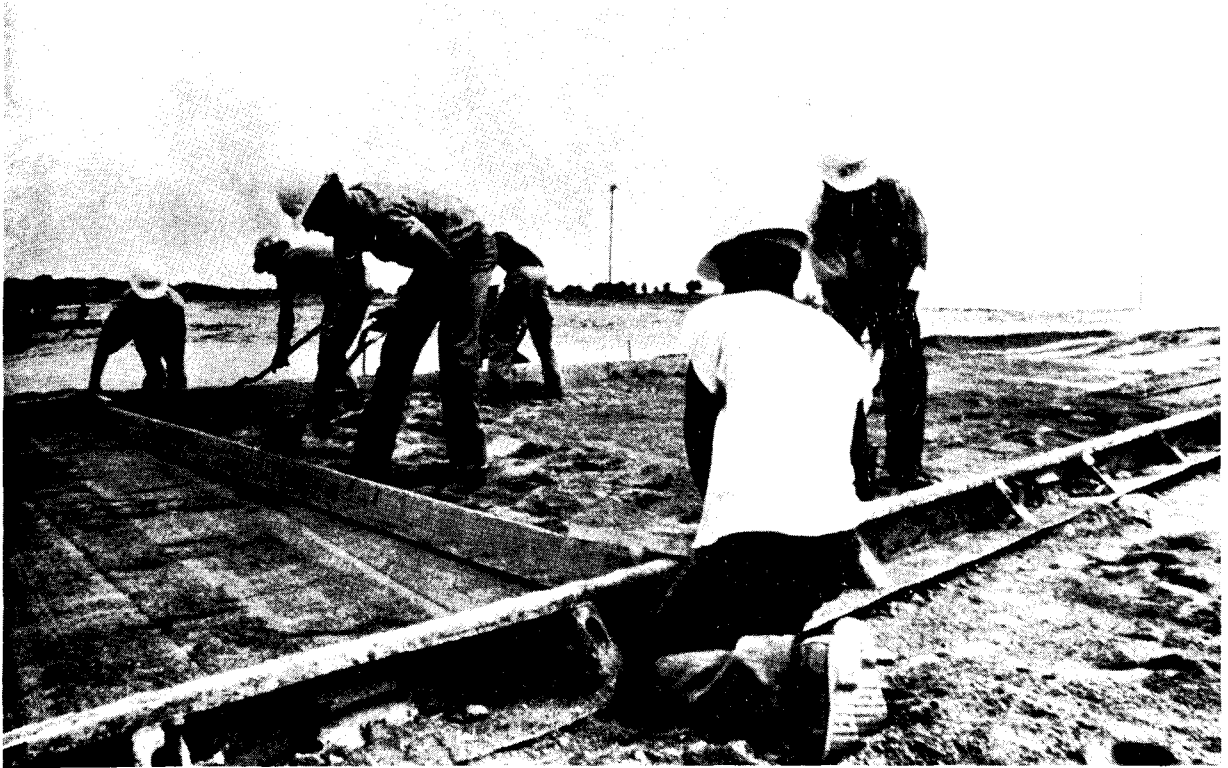


Figure 4: SETTING FORMS AND USING SAND FOR FINE GRADING OF SUB-GRADE



Figure 5: GLASS RIBERS ADDED TO READY-MIX AT THE JOB SITE

(#3 bars at 24-inch centers both ways) was placed. No chairs were used, but the reinforcement was pulled up into position at the middle of the slab depth when the concrete was placed.

Since the ready-mix plant was located some 15 miles (25 minutes) from the test site, the concrete which was to be reinforced with glass was brought to the site and the fibers were added on the job. See Figure 5. The proportions used for slabs # 2, 3, 4 and 5 included 6 sacks of cement per cubic yard, crushed lime stone aggregate of  $\frac{1}{2}$ -inch maximum size and the same sand as that used for the control slab. The mix design provided a 7" slump of the concrete before glass fibers were added.

The chopped glass fibers, 1" long, were dumped from 50 pound cardboard shipping containers directly into the hopper of the ready-mix truck. The truck mixer was then operated at maximum rotational speed for 3-5 minutes. Thorough distribution was achieved, and there was almost no evidence of any clumps or bunches of fibers being formed.

Slab #5 was first placed. The glass fiber content was 1.34 percent. At this volume fraction, the concrete was very stiff and did not readily eject from the mixer. Additional water was therefore added, 25 gallons to the 7 cubic yard batch, increasing the water/

cement ratio to 0.700. Even at this increased water content, the composite material was difficult to place and finish. See Figure 6. An electric Wyco vibrator was used to aid in compaction and placement, along with a vibrating screed. The finished surface of slab #5 was moderately rough with some small voids and irregularities.

The 7 cubic yard batches used for slab #4 and #3 also had water added in such an amount that the water/cement ratio became 0.688. The amount of glass fiber content was reduced to 0.97 percent by volume. At these proportions, the concrete was placed with relative ease. Vibration was, of course, still required.

The concrete crew foreman had additional water added to the concrete batches used for slab # 2. No appreciable increase in workability was realized and it was necessary to approximate the water/cement ratio at a value of about 0.800.

The finishing of slabs 2, 3 and 4 proved to be no problem. See Figure 7. A normal surface of texture that would provide standard skid resistance was provided.

Test specimens were taken from the concrete used in each slab. Three compressive cylinders and three beam specimens were cast. These test specimens were cured in a moist room at 90 percent humidity, 70<sup>0</sup> Fahrenheit, for 28 days. A summary of all batch proportions and the physical properties of the concrete as determined by





Figure 6: LOW SLUMP FIBER REINFORCED CONCRETE  
(AT  $\frac{V_r}{V} = 1.34\%$ ) REQUIRED EXTRA EFFORT IN PLACEMENT



Figure 7: PLACEMENT AND FINISHING WERE RELATIVELY  
EASIER AT  $\frac{V_r}{V} = 0.97\%$

test to failure are shown by Table 3-1.

Curing compound was applied and the test slabs were allowed to cure for 42 days. There were frequent, heavy rains during the curing period. Deflection tests described in Section 4 and the continued application of test loads were delayed from the planned date (July 24), when the pavement would have been curing for 28 days, to August 7. The delay would have no significant effect upon test results.

The rains did, however, erode the sand fill material at the edges of the 4-inch and 6-inch slabs. Forms were removed on July 6. Because of rain, the shoulders were not graded until July 18. The right side (Easterly edge) of Slab #5 was broken by the tractor/loader that was placing shoulder fill material. Some of the other early edge failures of Slabs #3 and #4 may have been the result of lack of edge support.

TABLE 3-1  
 BATCH PROPORTIONS AND PHYSICAL PROPERTIES OF  
 CONCRETE TEST SLABS

Slab No.	Agg Size	Cement lbs/yd <sup>3</sup>	W/C	f' <sub>c</sub> lbs/in <sup>2</sup>	f <sub>r</sub> lbs/in <sup>2</sup>	Reinforcement
1	1½"	470	0.650	3207	624	#3Ø bars @ 24" o. c.
2	½"	564	0.800*	1373	575	0.97% glass fiber vol.
3	½"	564	0.688	2479	749	0.97% glass fiber vol.
4	½"	564	0.688	2630	732	0.97% glass fiber vol.
5	½"	564	0.700	1250	849	1.34% glass fiber vol.

\* Water added for workability approximated

## SECTION 4

### DEFLECTION MEASUREMENTS

On August 7, 1973, deflection measurements were taken, on the test slabs described in this report, after 42 days of curing. Deflections were measured on each of the test slabs except for Slab #5, which had suffered distress during the shoulder grading operations. Deflections were measured under both static and dynamic load conditions.

The loads were applied by a Euclid rock hauler, with an empty weight of 58,300 pounds, loaded with rock weighing 70,000 pounds. See Figure 8. Loaded, the front axle carried a load of 43,100 pounds or 21,550 pounds per front wheel. The rear axle carried a load of 85,200 pounds or 21,300 pounds per rear wheel. The static deflections were measured with the load at the following three positions:

- 1) Load Position #1:  
Rear wheels just at the edge of the slab and the front wheels on the slab, just forward of the center of the slab.
- 2) Load Position #2:  
Centroid of loaded truck over the mid-point of the slab.
- 3) Load Position #3:  
Rear wheels directly over the mid-point of the slab, with the front wheels upon the next slab.

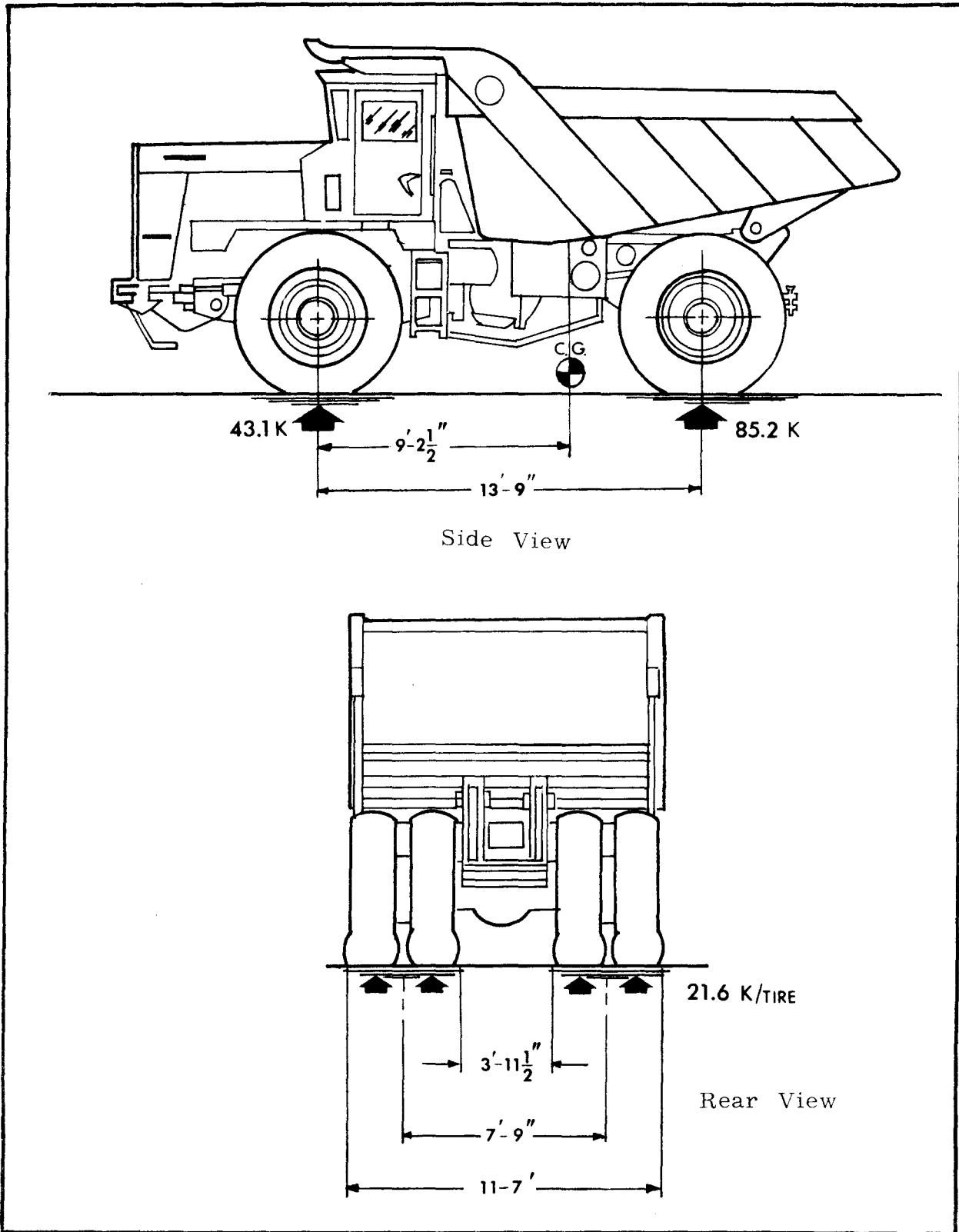


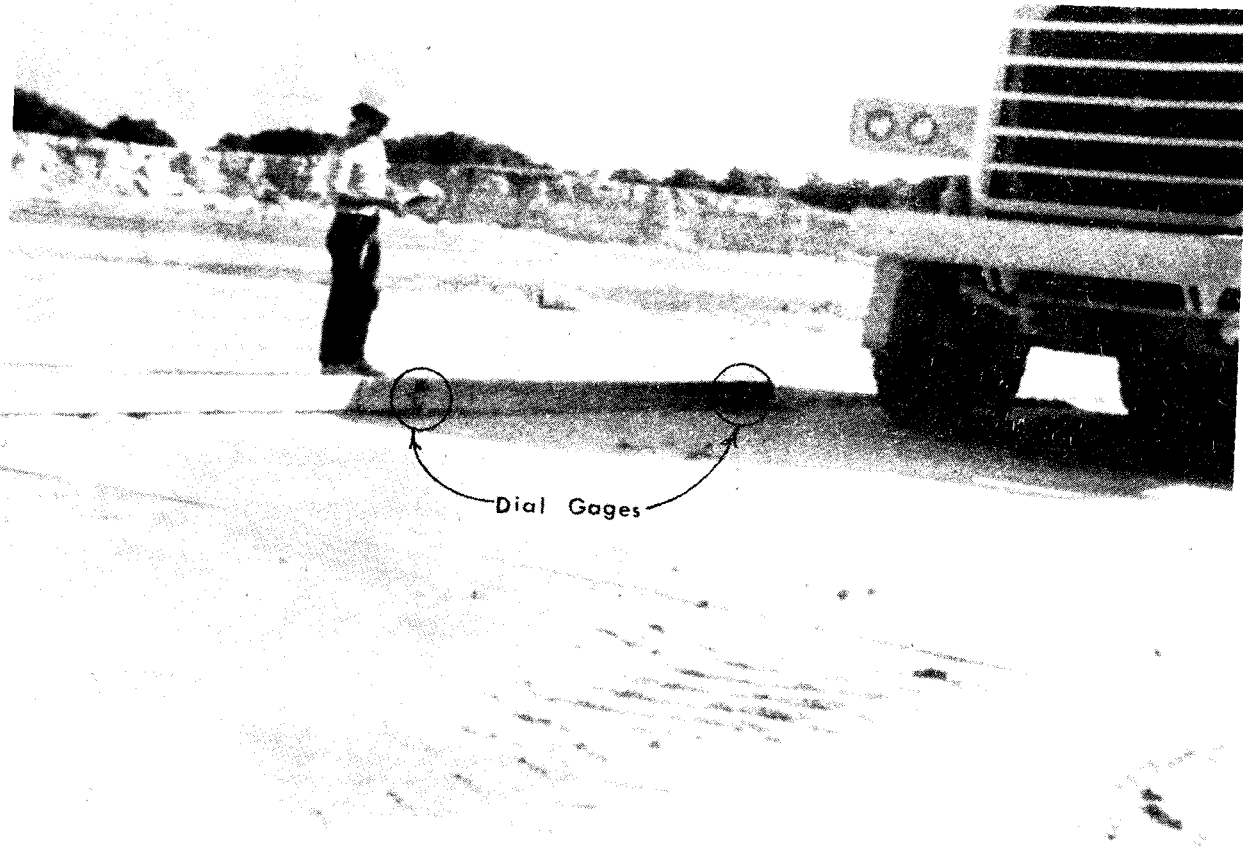
Figure 8: EUCLID ROCKHAULER, TEST LOAD VEHICLE

Dynamic deflections were measured as the truck drove over the slab at a velocity of about 20 miles per hour.

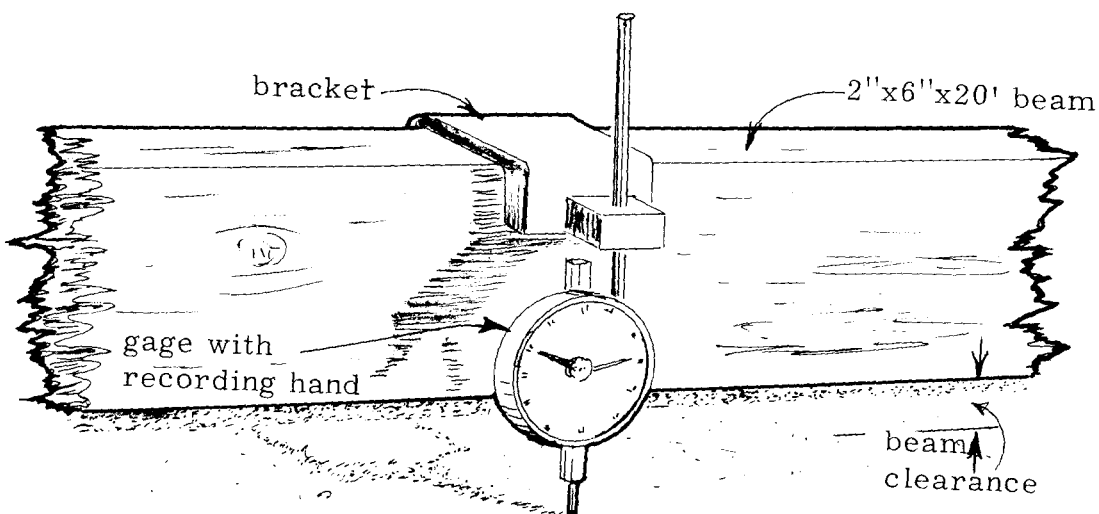
Dial gages were mounted on a 2 x 6 inch beam of Douglas Fir, twenty-two feet long, as shown by Figure 9. Each end of the beam was supported on the adjacent slab on  $1\frac{1}{2}$  inch chairs. Therefore, the gages were in no way connected to the slab under observation. The dial gages used provides for readings to the nearest 0.01 inch and had a maximum recording hand.

Measurements for both the static and dynamic deflections were taken with a gage at the front edge, midpoint, and rear edge of the slab, as shown by Figure 10. The gages were positioned longitudinally along the slab at the right edge, the center line and the left edge. The procedure used to take measurements was as follows:

- 1) The gages were set up along the left edge and zeroed, with no load on the slab.
- 2) A loaded vehicle was then driven upon the slab and stopped with the rear tire print just on the front edge of the slab. Deflections were recorded for Load Position #1.
- 3) The truck was then moved up until the centroid of the loaded truck was directly over the midpoint of the slab. The centroid is shown by Figure 8 to be 9.2 feet back from the front hub. The deflections were recorded for Load Position #2.
- 4) The loaded truck was then moved up to stop with the rear tire print aligned laterally with the midpoint of the slab.



(a) Loaded Euclid in position for deflection measurement.



(b) Dial gage and reference beam.

Figure 9: SET-UP FOR DEFLECTION MEASUREMENTS.

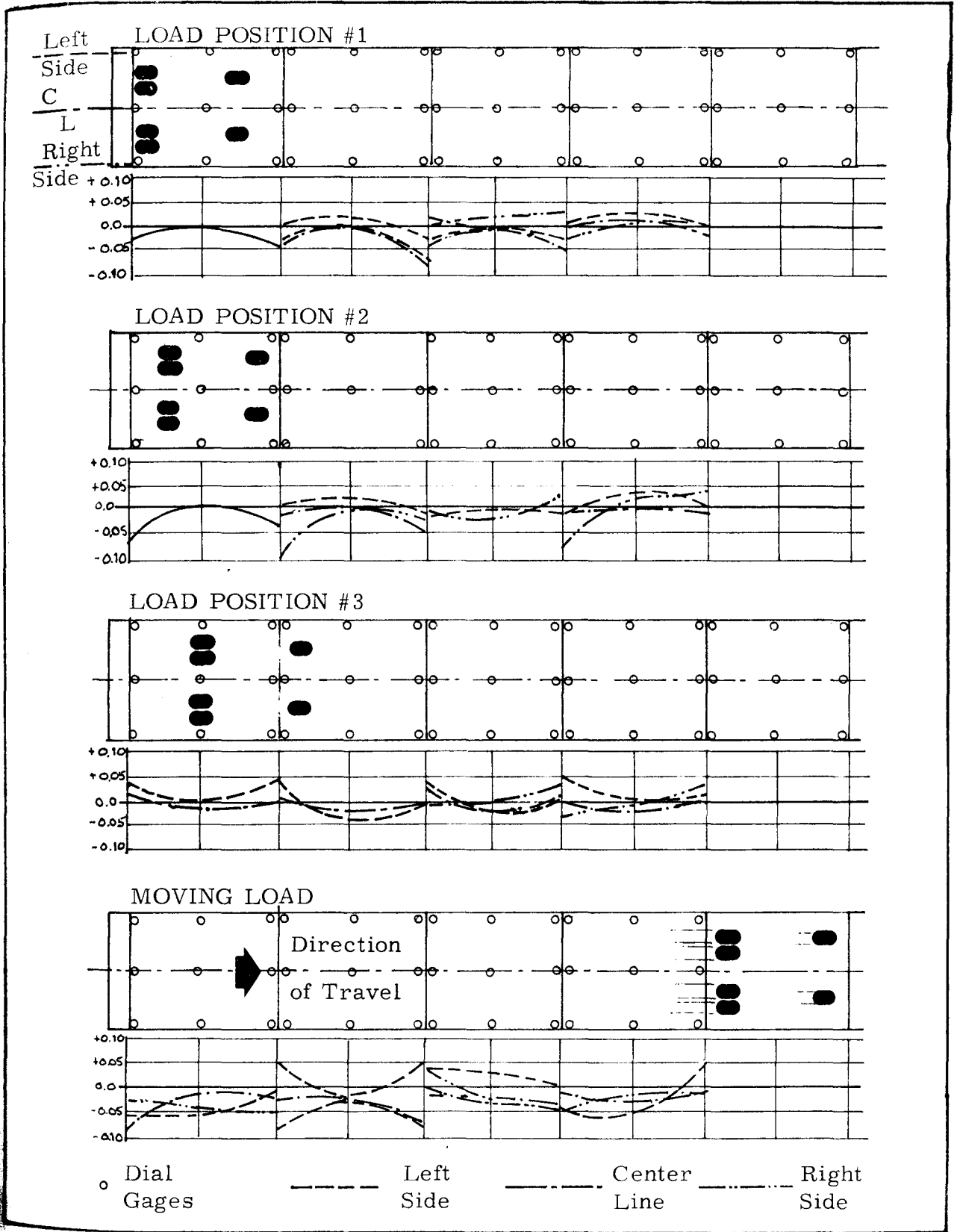


Figure 10: DEFLECTION MEASUREMENT



The front wheels were off the slab, supported by the next slab in the direction of travel. Deflections were recorded for Load Position #3.

- 5) The truck was then driven off the slab, leaving it unloaded. The gages were zeroed and the maximum recording hand set. The truck was then driven across the slab at a speed of about 20 miles per hour applying a dynamic load. The readings as shown by the maximum recording hand were recorded.
- 6) Next, the gages and supporting frame were moved to the center line of the slab and the procedure repeated. After a complete set of static and dynamic readings, the same procedure was used for the right edge of the pavement slab.
- 7) The procedure was repeated in the same sequence for left, center line, and right edge for each slab in turn.

During the dynamic tests, as the truck passed over the slab, both upward and downward deflections were noted. However, the maximum recording hand would record only negative (downward) deflections. Under the moving loads, the positive deflections along the edge where the gages could be seen were approximated and recorded by an observer stationed at each gage. Of course, this could not be done for center line readings. Therefore, for edge points, it was possible to record both positive and negative deflections; while on center line, only negative movements were taken.

Slab #5 showed serious distress after six loads had passed over it. This slab was broken off along one edge by the machine used

to grade the shoulders. The absence of the entire right edge of Slab #5 resulted in some difficulty in supporting the beam for right edge measurements of Slab #4. However, with care taken, compatible measurements were made.

The deflection measurements permit an approximation of the stresses induced at edges and at center line, parallel to the direction of travel of the test load vehicles. If a uniformly varying sub-grade reaction can be assumed, the deflection

$$\delta = \frac{WL^3}{15EI} \quad ,$$

and the effective total sub-grade force

$$W = \frac{15EI\delta}{L^3}$$

where L is the effective bending length, taken to be half of the slab length, or 120 inches. The modulus of elasticity varies, as shown by Table 6-2:

- 1) Slab #1,  $E = 3.23 \times 10^6$
- 2) Slab #2,  $E = 2.17 \times 10^6$
- 3) Slab #3,  $E = 2.92 \times 10^6$
- 4) Slab #4,  $E = 3.01 \times 10^6$

The moment of inertia for a strip of 12 inch width along the edges and

along the center line

$$I = t^3 \quad ,$$

where  $t$  is the pavement thickness.

The bending moment induced by the loads is

$$M = \frac{2WL}{3} = \frac{10EI\delta}{L^2}$$

and stress

$$f_r = \frac{10EI\delta t}{2L^2 I} = \frac{5E\delta t}{L^2}$$

The indicated stresses thus calculated, and discussed in Section 6, are not the maximum stresses. These would occur directly under the tire imprint area. However, the calculated stresses induced by static loads, which range from 448 psi in Slab #1 to 420 psi in Slab #4, verify the order of magnitude of the stresses calculated by the PCA method or the AASHO method.

## SECTION 5

### OBSERVED PERFORMANCE

The application of loads to the test pavement slabs was begun on August 7, 1973, as shown by Figure 11, and continued with periodic observations made through March 15, 1974. For observing and recording the developing crack pattern, the pavement surface was swept clean (see Figure 12). Extension of cracking was carefully mapped.

The measurement of deflections under static and moving loads, discussed in the previous section of this report, required 13 repetitions of the test loads. At this point, the cracking of Slab #5 had progressed to a terminal condition. The right-hand (northerly) corner of Slab #4 was also showing considerable distress. A single crack, running laterally across the slab, was seen in the conventionally reinforced Slab #1. As shown by Figure 13, glass fiber reinforced Slab #2 and #3 evidenced no distress.

After removal of Slab #5, routine loading was resumed. The results of periodic mapping of cracks are tabulated in Table 5-1. Crack growth proceeded rapidly in Slab #4. It was determined that the failure of the Northeast corner of Slab #4 was due, in part, to the deposition of the residue from Slab #5 batch at the time of initial pouring. In any case,



Figure 11: FIRST TEST LOAD APPLIED



Figure 12: SWEEPING PAVEMENT TO EXPOSE CRACK PATTERN

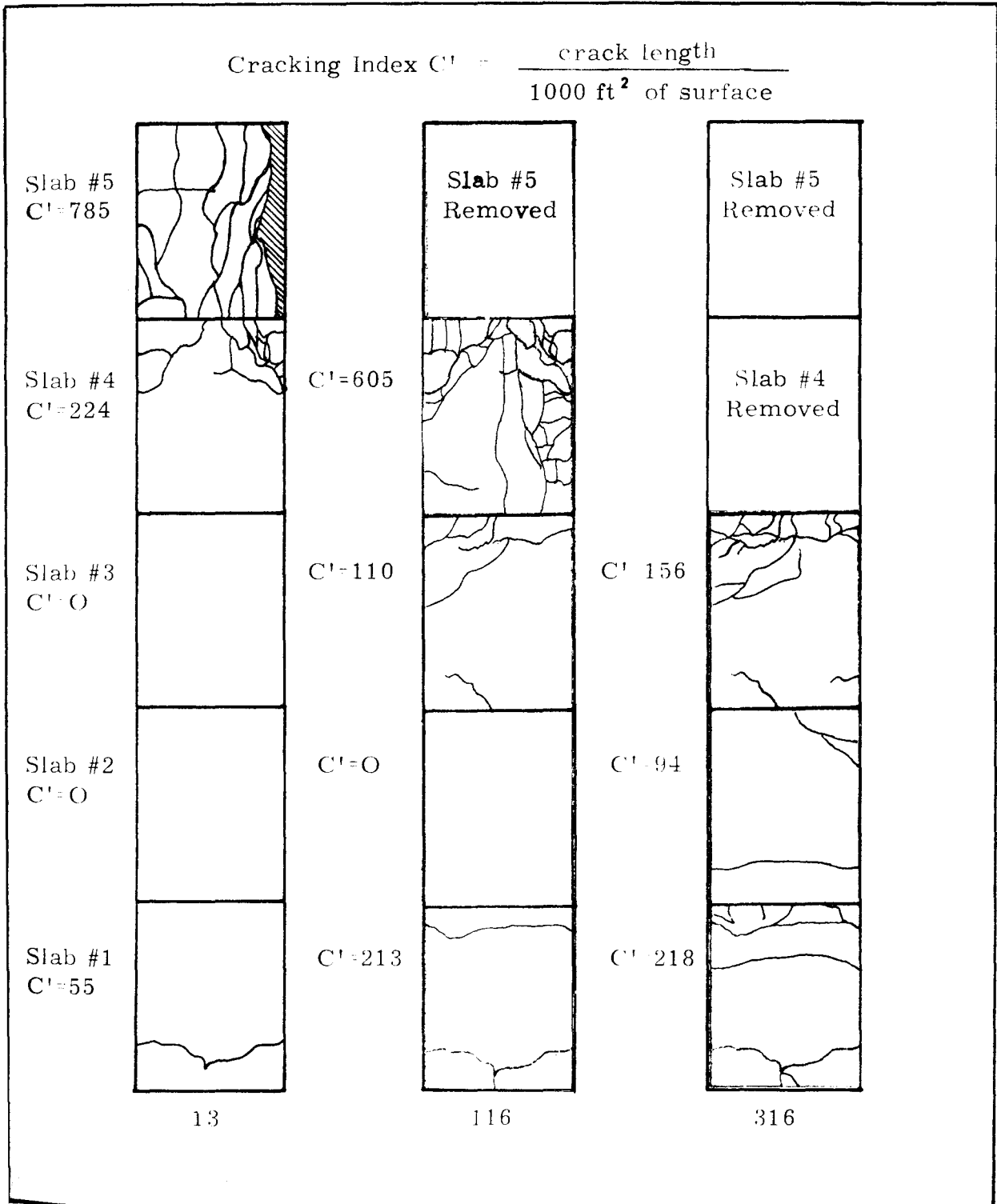


Figure 13: CRACK DEVELOPMENT UNDER 85 KIP SINGLE AXLE TEST LOADS

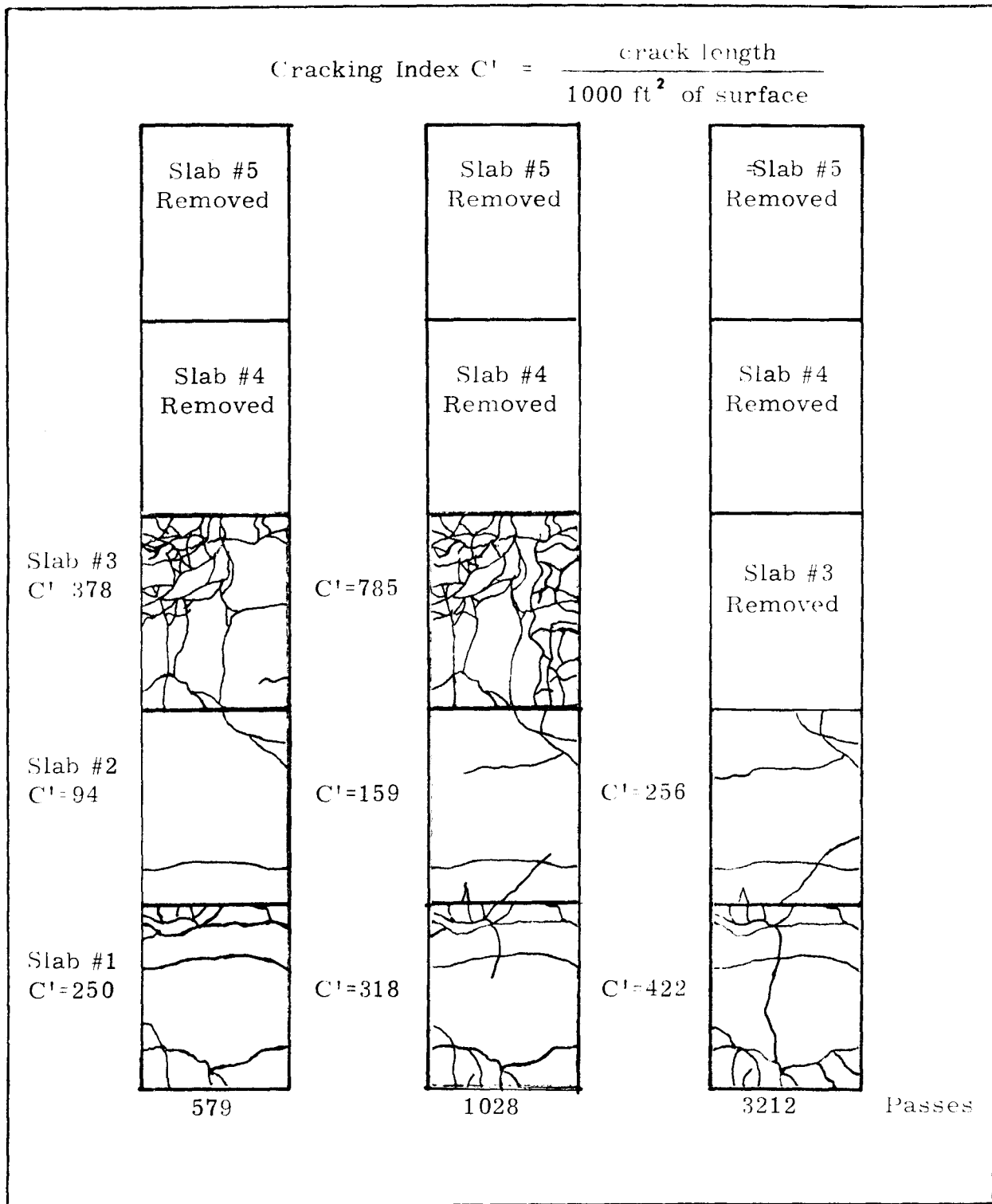


Figure 14: CRACK DEVELOPMENT UNDER 85 KIP SINGLE AXLE TEST LOADS

the 4-inch, glass fiber reinforced Slab #4 had reached a terminal condition 116 load repetitions. It was also noted that, at this point, Slab #3 had developed the same amount of cracking as the control slab. In other words, up to this point, the 6-inch glass fiber reinforced slab had performed better than the conventional steel reinforced Slab #1.

TABLE 5-1  
CRACK DEVELOPMENT  
(Crack Length in inches)

Slab No.	Load Repetitions - 85 kip Axle Load								
	13	20	116	179	316	578	678	1028	3212
1	17	20	35	68	70	80	90	102	135
2				30	30	30	30	53	82
3		15	35	50	50	121	150	250	Terminated
4	72	108	193	Terminated					
5	250	Terminated							

At about 400 load repetitions, the cracks in Slab #3 began to develop more rapidly than did those of Slab #1. It continued in service up to 1028 passes. Figure 15 shows the condition of Slabs #1, #2, and #3 at this point of the test. Slab #3 was then removed and loads were



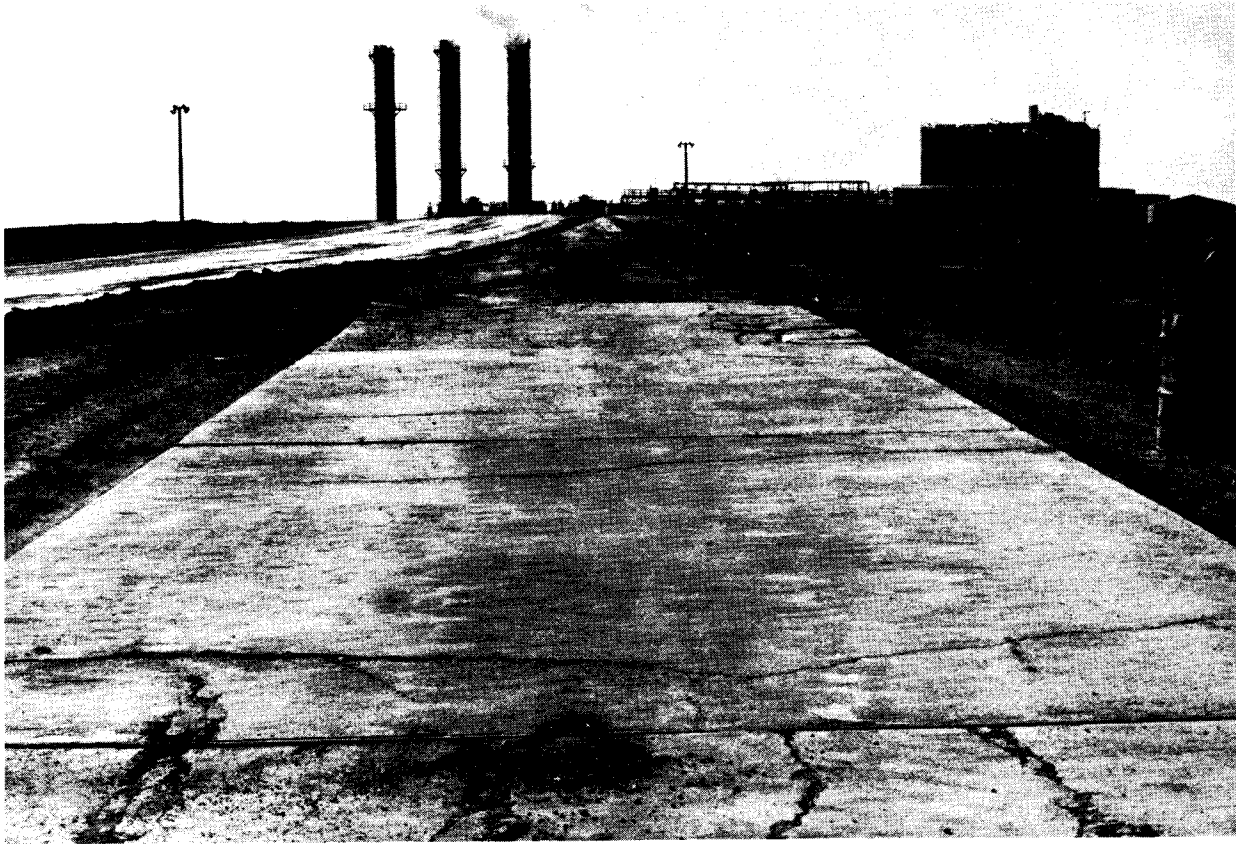


Figure 15: SLABS #1, #2, AND #3 AFTER 1028 LOAD REPETITIONS

applied, continuing to 3212 repetitions on March 15, 1974.

At the conclusion of the formal observations, a stable condition appears to have been reached. Minor growth of crack pattern is continuing with the glass reinforced Slab #2 performing somewhat better than the conventional Slab #1. See Figure 16. The two slabs will continue in service, under loads, until one or the other reach a terminal condition.

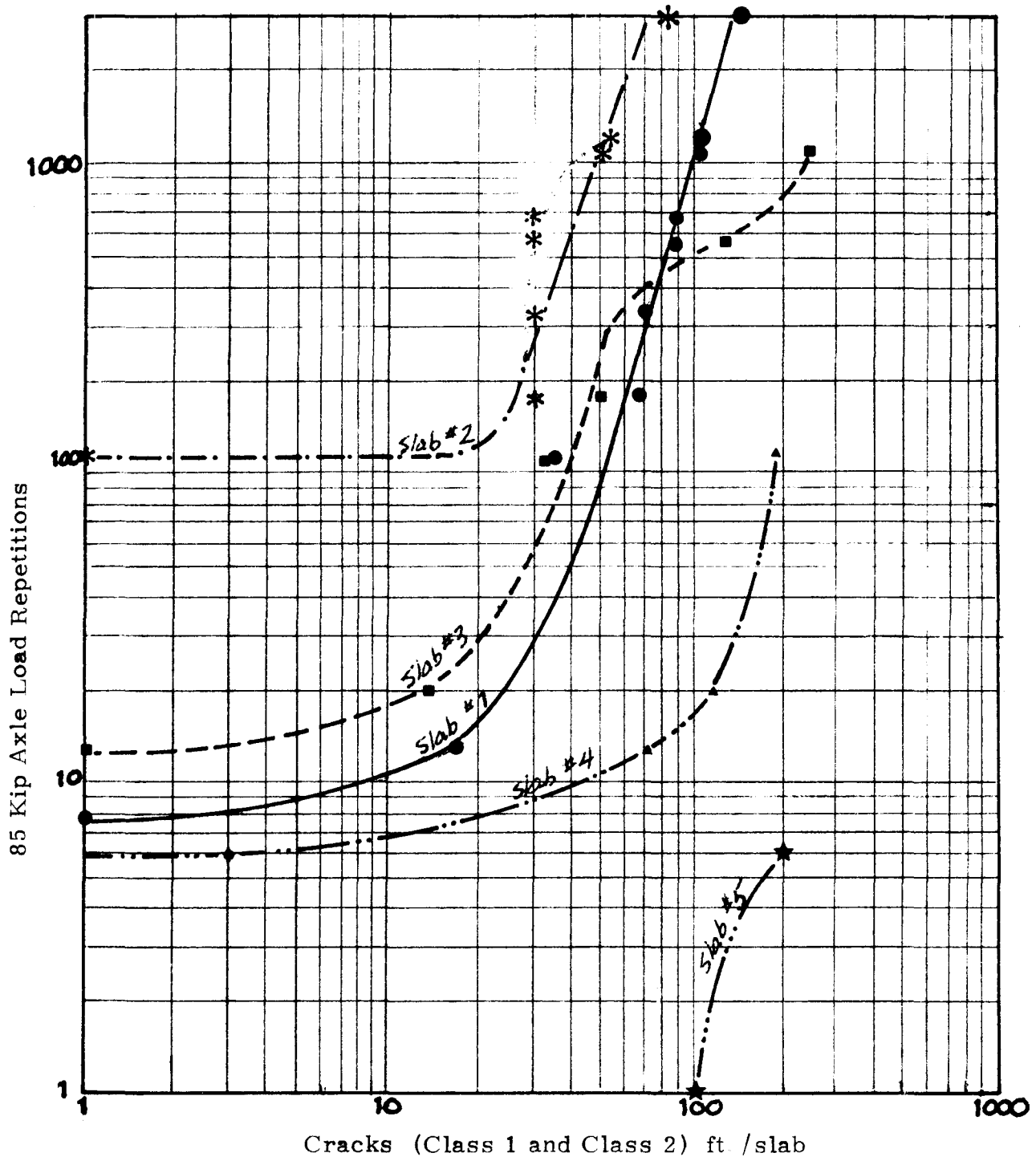


Figure 16: PAVEMENT TEST SLAB PERFORMANCE

## SECTION 6

### PERFORMANCE EVALUATION

Rigid concrete pavements for airports, highways and municipal streets are subject to repetitive loadings induced by traffic and, sometimes, by cyclic shrink/swell phenomenon associated with the sub-grade. The mechanism of failure is primarily that of fatigue. Conventional steel bars, placed at the middle of the cross-section (the neutral axis) in municipal pavements, is ineffective as reinforcement for flexural stresses. The conventional reinforcement is also relatively ineffective for shear stresses and primarily acts as a means of load transfer across cracks and across construction joints.

When cracks form and propagate a pavement is not necessarily rendered unserviceable. The sub-grade provides continued support unless there is some secondary effect, such as pumping, that results in excessive deflection.

The principal methods for the design of pavements are the Portland Cement Association (PCA) method, or the technique advocated by the Association of State Highway Officials (AASHO). Modifications of the Westergaard theory provide the basis for the PCA method. The AASHO Road Test, an in-depth field investigation, provided the basis

for the AASHO method. The results of the accelerated field trials on the municipal pavements reported herein have been evaluated in terms related to both of these design concepts.

#### 6.1 Serviceability Performance Analysis:

By AASHO definition, Present Serviceability is a measure of the ability of a pavement to serve its function as a highway or street surface, subject to vehicular traffic. The assessment of a pavement to determine its Present Serviceability Index (p) can be done either by observation of ride quality and surface condition or by taking measurement of surface slope variations (SV) and its cracking index (C') in lineal feet of crack per 1,000 sq. ft. of pavement area. The adjective scale that has been adopted by AASHO<sup>(1)</sup> to indicate relative serviceability is as follows:

- 1) A "very good" pavement ranges in values of p from 4.0 to 5.0.
- 2) A "good" pavement has p values from 3.0 to 4.0.
- 3) For a "fair" pavement surface, p ranges from 2.0 to 3.0. At a serviceability index of 2.2 to 2.5, a rigid pavement is taken to be ready for resurfacing.

---

(1) Bartelsmayer and Finney, "Use of AASHO Road Test Findings by the AASHO Committee on Transport". Highway Research Board Special Report 73, Proceedings of a conference held May 16-18, 1962, St. Louis, Mo.

- 4) A "poor" pavement has a serviceability index,  $p$ , of 1.0 to 2.0. At  $p=1.5$ , a rigid pavement is in terminal condition.
- 5) "Very poor" pavements, with  $p$  values of 0.0 to 1.0, would be unuseable for all practical purposes.

For the service test slabs described herein, each slab was subjected to traffic until it had reached a terminal condition. A value of  $p=1.5$  is taken to be that point at which a failed slab was removed so that the loading of remaining slabs could continue.

Test loading was provided by large, loaded, Euclid rock-hauling vehicles of a gross vehicle weight of 128,300 lbs. The front axle load was 43,100 lbs. and the drive axle was 85,200 lbs. Details of the test vehicle are shown and discussed in Section 4. For determining the equivalent effects of load repetitions of this magnitude, the procedure described by the Highway Research Board Special Report 73 was used.

The basic AASHO Road Test Equation<sup>(2)</sup> is

$$G_t = \log \frac{C_o - p}{C_o - 1.5}$$

where  $G_t$  is the logarithm of the ratio of loss in serviceability, at time  $t$ , to the potential loss taken to the point where  $p=1.5$ .  $C_o$  is the

---

(2) Langsner, Huff and Liddle, "Use of Road Test Findings by AASHO Design Committee", op. cit.

initial serviceability index, taken for this test to be 4.5.

For single axle load repetitions, the equivalence factor for a given magnitude of the single axle load,  $y$  in kips, is compared to the relative effect of a single axle 18 kip load by

$$W_{t_{18}}/W_{t_y} = 4.62 \log (y+1) - 4.62 \log (18+1) + G_{t/B_{18}} - G_{t/B_y},$$

where  $W_{t_y}$  is the number of load repetitions of an 18 kip single axle load producing the same effect as the test load repetitions  $W_{t_y}$ , and where  $y$  is the magnitude of the test load that is taken to be 85 kips in the test reported here. For a single axle test load, the value of  $B$  is determined by

$$\log (\beta - 1.0) = \log 3.63 + 5.20 \log (L_1 + 1.0) - 8.46 \log (D + 1),$$

where  $L_1$  is the magnitude of the axle load (the same as  $y$  in the previous equation) and  $D$  is the depth of the pavement in inches.

Using the given equations, values of  $\beta$  were found for the basic single axle load of 18 kips and for depths of 4, 6, 8, and 10-inches. Similar values of  $\beta$  were found for a single axle load of 40 kips, the upper limit of equivalence factors calculated and previously reported by others<sup>(3)</sup>. The equivalence factors  $W_{t_{18}}/W_{t_{40}}$  were verified as shown in Table G-1 and are plotted, for various

---

(3) Langsner, Huff and Liddle, op. cit.

serviceability indices, and pavement depths, in Figure 17.

For the test loads actually used (85 kip axle loads), equivalence factors were calculated and are also tabulated in Table 6-1. In Figure 18, the equivalence factors are plotted versus pavement depths for various values of serviceability index  $p$ . It can be seen that when test loads were applied until the pavement reached a terminal condition,  $p=1.5$ , each load repetition by a loaded Euclid has the equivalent effect of 1070 load repetitions by a single axle load of 18 kips.

TABLE 6-1  
EQUIVALENCE FACTORS

D	(p = 2.5)		(p = 2.0)		(p = 1.5)	
	$W_{18}/W_{40}$	$W_{18}/W_{85}$	$W_{18}/W_{40}$	$W_{18}/W_{85}$	$W_{18}/W_{40}$	$W_{18}/W_{85}$
8	25.65	750.2	30.41	911.3	34.93	1070
6	30.61	884.8	32.18	961.4	34.93	1070
4	34.27	1051	34.63	1062	34.93	1070

Figure 19 summarizes the equivalence factors, for a range of axle loads from 18 kips to 100 kips, for degradation of serviceability

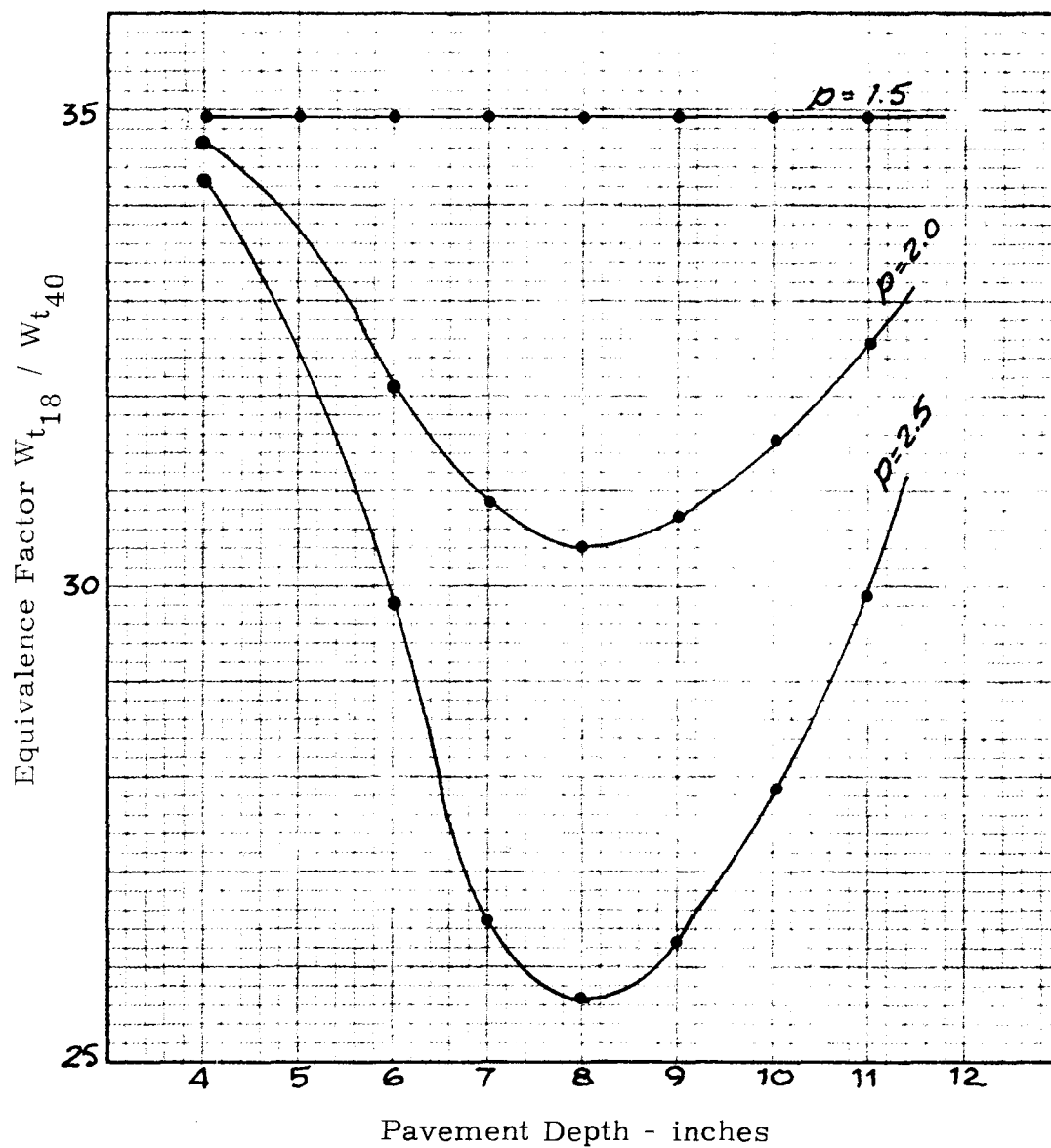


Figure 17: EQUIVALENT 18 KIP AXLE LOAD REPETITIONS  
PRODUCED BY 40 KIP AXLE LOADS



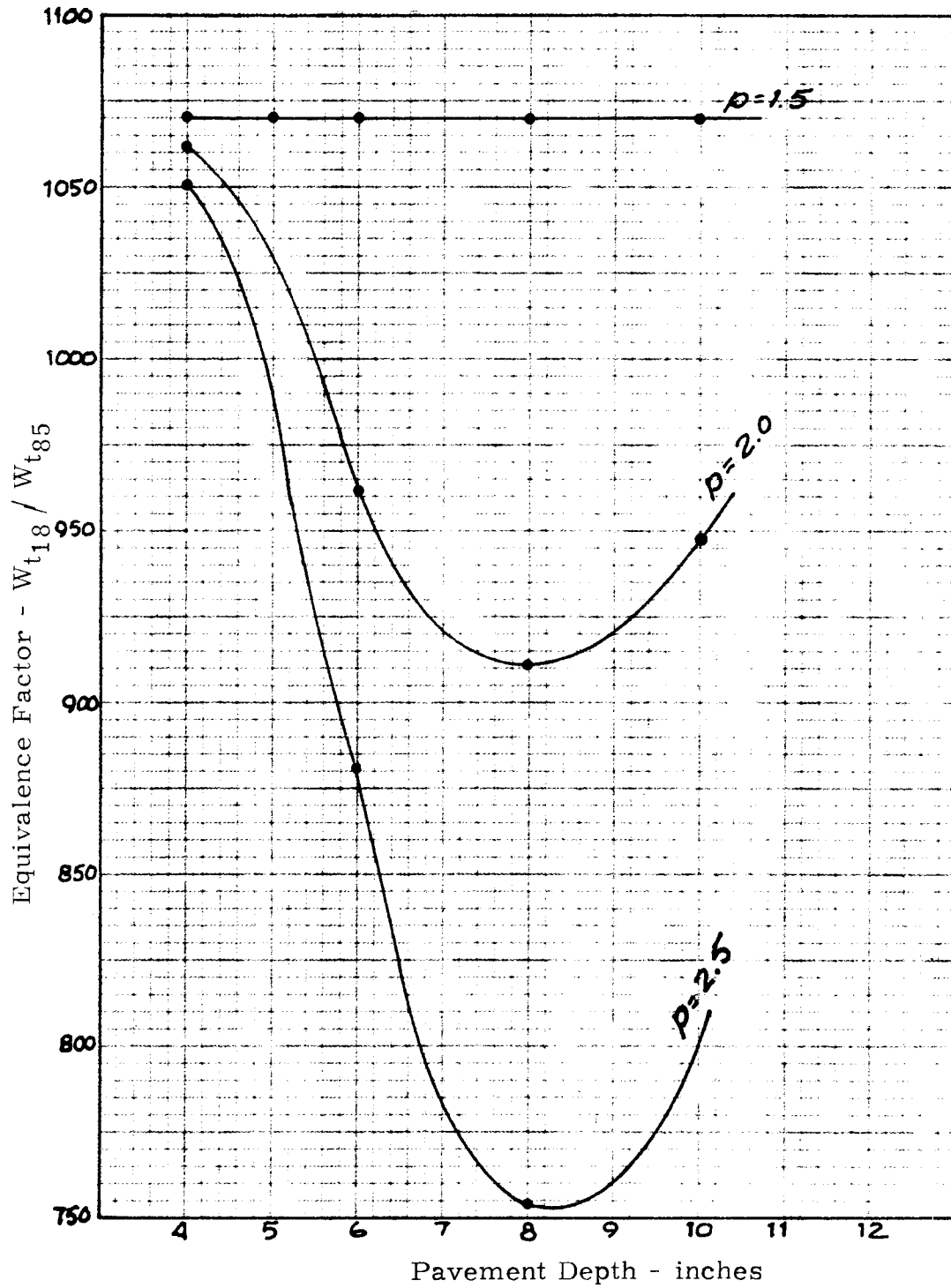


Figure 18: EQUIVALENT 18 KIP AXLE LOAD REPETITIONS  
PRODUCED BY 85 KIP AXLE LOADS

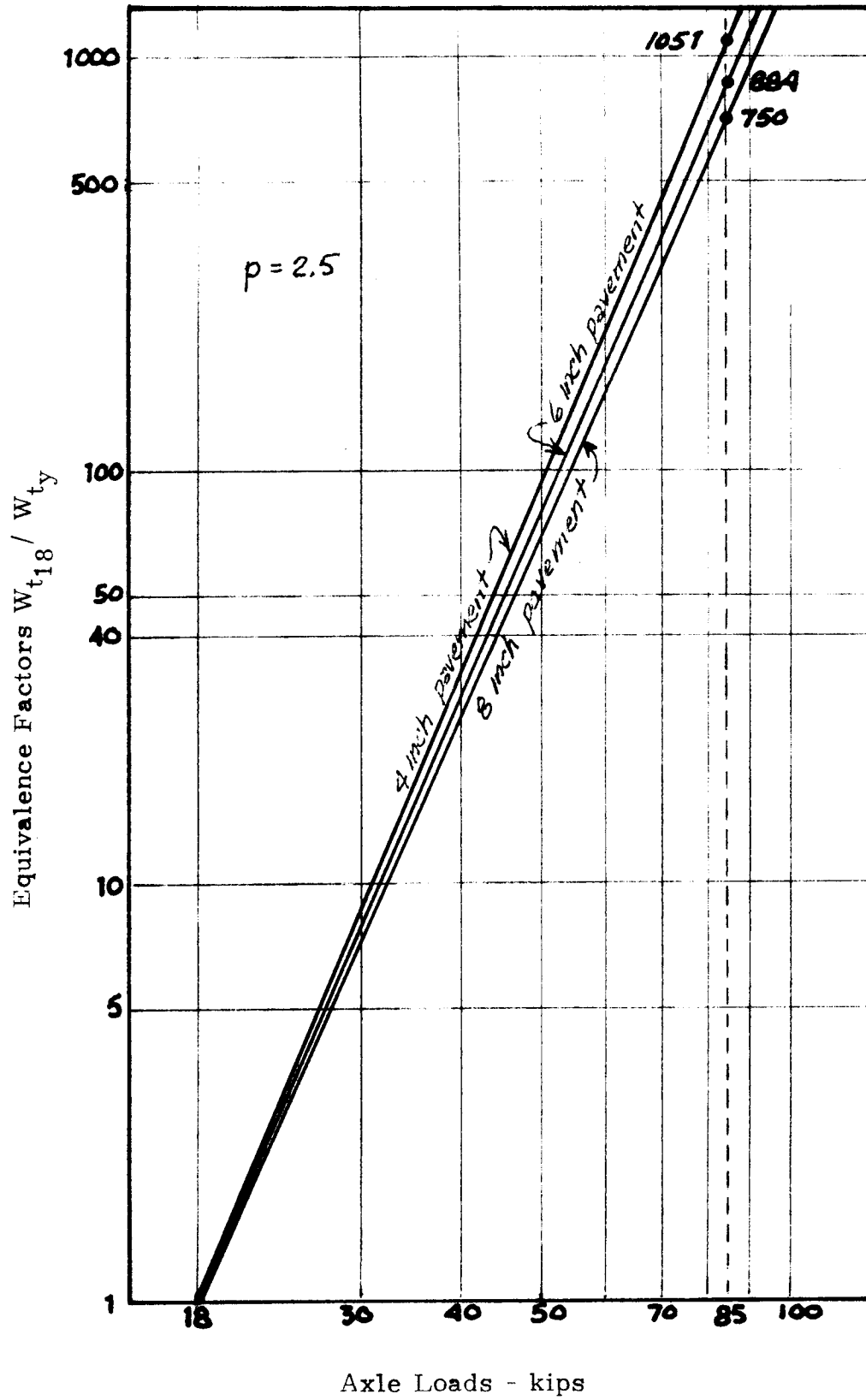


Figure 19: RELATIVE EFFECT OF AXLE LOAD REPETITIONS COMPARED TO 18 KIP AXLE LOAD

from 4.5 to 2.5. The log-log relationship for degradation to 1.5 converges upon an equivalence factor of 1070 for an 85 kip single axle load. The AASHO design criteria, thus provides the means for quantitative assessment of the performance of the glass fiber reinforced pavement slabs as well as comparative assessment with respect to the performance of the control slab.

#### 6.2 Flexural Stress Analysis:

The PCA method of design for rigid pavements is based upon theoretical studies of pavement slab behavior by Westergaard, Pickett, and others.<sup>(4)(5)(6)</sup> The method permits stress computations for multiple wheeled vehicle configurations with consideration given to sub-grade support, axle and wheel loads, and slab thickness. These parameters are used to determine the flexural stress development in the concrete. The magnitude of this stress is then compared to the ultimate flexural strength of the concrete, and

- 
- (4) Westergaard, H. M., "Stresses in Concrete Pavement Computed by Theoretical Analysis", Public Roads, Vol. 7, No. 2, April '26.
  - (5) Pickett and Ray, "Influence Charts for Concrete Pavements", American Society of Civil Engineers Transactions, Paper 2425, Vol. 116, 1951.
  - (6) Pickett, Raville, Jones and McCormick, "Deflections, Movements, and Reactive Pressures for Concrete Pavements", Kansas State College, Bulletin 65, October 1951.

stresses greater than 50% of the ultimate are considered to be of increasing significance as value of the stress ratio approaches 1.0. In other words, light vehicle loads which stress the pavement up to 50% of its modulus of rupture are assumed to have negligible effect upon the life of the pavement. The number of heavy load repetitions, that produce stress ratios  $f_r/f'_{r} \geq 0.50$ , are considered as the criteria for predicting the fatigue life of the pavement which is reached when the pavement shows its first structural crack.

For the prediction of the performance of the test slabs described in this report, the stresses at the pavement edge were taken as critical.<sup>(7)</sup> At maximum gross weight (fully loaded) the Euclid vehicle tires carry 22.6 kips each on the drive axle and 21.6 kips each on the front axle with a contact pressure of 70 psi. A contact area of 323 in<sup>2</sup>/tire was calculated for the drive axle tires and 309 in<sup>2</sup>/tire for the front.

The relatively small difference between front and drive axle tire loading proved to be negligible, and the contact area was taken to be

$$L = \sqrt{\frac{323}{0.5227}} = 24.8 \text{ inches, and}$$

---

(7) "Load Stresses at Pavement Edge", a supplement to "Thickness Design for Concrete Pavements", Portland Cement Association, Bulletin 1S030.01P, Skokie, Illinois, 1969.

$$W = 0.6L = 14.9 \text{ inches.}$$

Attention is invited to Figure 20.

Westergaard postulated that the stress in a pavement is a function of a term called the "radius of relative stiffness" ( $l$ ) which is a measure of the ratio of the rigidity of the concrete pavement to the rigidity of the subgrade, and

$$l = \sqrt{\frac{Ed^2}{12(1-\mu^2)k}}$$

The introduction of glass fibers to the concrete matrix contributes to a small increase in the elastic modulus, ranging from 1.6 to 3 percent.<sup>(8)</sup> The modulus of elasticity can be taken to be  $E = K_e 57000 \sqrt{f'_c}$ , where  $K_e$  is the coefficient taken to be 1.03 for glass fiber reinforced concrete. The adjusted values for  $E$  and of  $l$  were, therefore, calculated and are tabulated in Table 6-2 for each pavement slab tested.

With the radius of relative stiffness determined, scale factors were calculated for dimensioning contact imprints for the tire arrangement that was shown by Figure 20. Using a small scale

---

(8) Buckley, E. L., Investigations of Alternative Fiber Reinforcements for Portland Cement Mortar and Concrete, Construction Research Center, TR-2-72, University of Texas at Arlington, November 28, 1972.

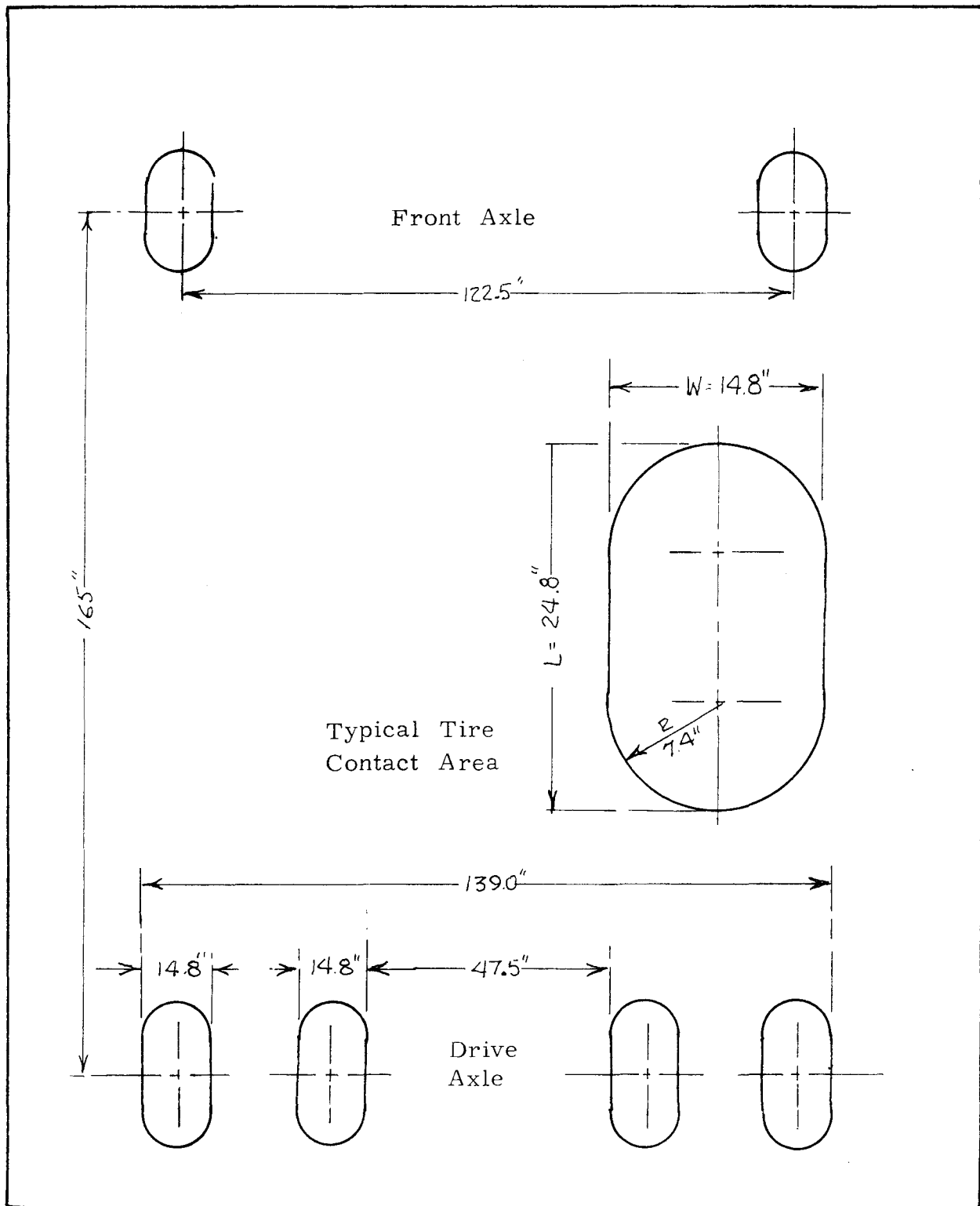


Figure 20: TIRE SPACING AND CONTACT AREA ON EUCLID TEST LOAD VEHICLE

Table 6-2

## RADI OF RELATIVE STIFFNESS

Slab No.	Depth (in.)	$f'c$ (lbs/in <sup>2</sup> )	$E_1$ (lbs/in <sup>2</sup> x10 <sup>6</sup> )	$K_e$	$E$ (lbs/in <sup>2</sup> x10 <sup>6</sup> )	$\mu$	$(1-\mu^2)$	$\ell$ (in.)
1	8	3207	3.23	1.00	3.23	0.18	0.97	24.41
2	8	1373	2.11	1.03	2.17	0.22	0.95	22.21
3	6	2479	2.84	1.03	2.92	0.19	0.96	19.23
4	4	2630	2.92	1.03	3.01	0.19	0.96	14.30
5	4	1250	2.01	1.03	2.07	0.22	0.95	13.05

influence chart, the tire imprint for a dual, drive wheel arrangement was superimposed as shown by Figure 21. With relative small values for  $\ell$ , the dimensions of the dual-wheel imprint area are large, indicating that the front wheels and the other set of duals have negligible influence upon the moment (and thus stress) at the critical point "O" at the edge of the slab.

Using an imprint overlay, scaled to the relative radius of relative stiffness, for each pavement slab, the number of blocks

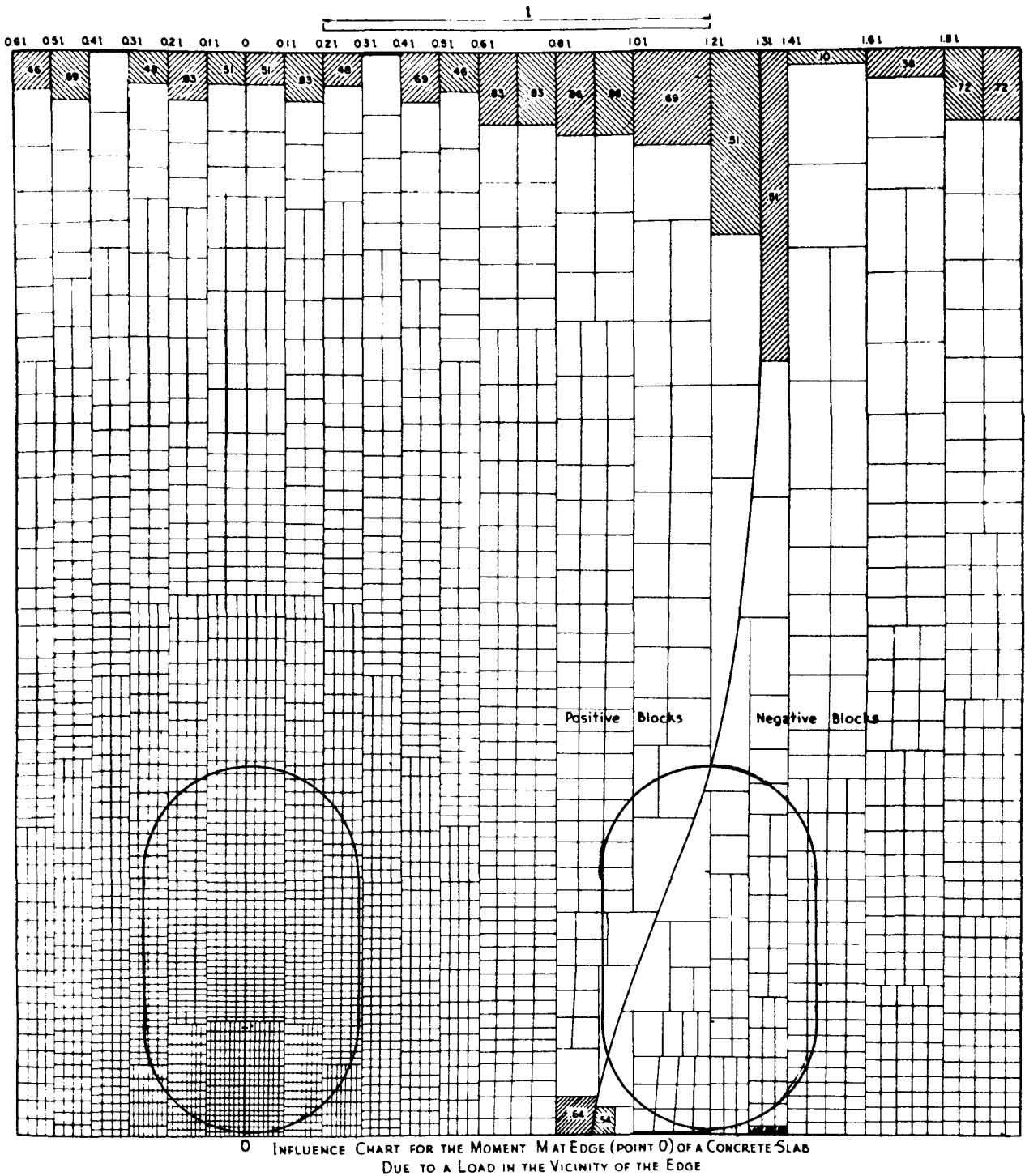


Figure 21: INFLUENCE CHART FOR MAXIMUM MOMENT (Pt. O)  
DUE TO EDGE LOADING.



Table 6-3  
MOMENT, STRESS AND STRESS RATIOS

Slab No.	N	$\rho$ (inches)	M (in. lbs)	$f_r$ (lbs/in <sup>2</sup> )	$f'_r$ (lbs/in <sup>2</sup> )	Stress Ratio	Allowable Repetitions
1	998	24.41	5010	470	624	0.75	490
2	1053	22.21	4541	426	575	0.74	650
3	1397	19.23	4361	727	749	0.97	1
4	1406	14.30	2426	910	732	1.24	0

covered on the influence chart were counted and added algebraically.

The equation for moment is:

$$M = \frac{q\rho^2 N}{10,000}$$

where  $q$  is contact pressure,  $\rho$  is the radius of relative stiffness, and  $N$  is the block count. The flexural stress

$$f_r = \frac{6M}{d^2}$$

Stresses were calculated, as indicated by Table 6-3, then compared to ultimate flexural strength that had been determined by test and

reported herein in Section 3. Stress ratios  $f_r/f'_r$  were then determined.

The calculation of stress can also be done by employing design charts presented by the Portland Cement Association in "Thickness Design for Concrete Pavements", PCA Bulletin ISOIO.O2P. However, the chart for a single axle load provides only for loads of up to 50 kips per axle. In Figure 22, the basic chart, arbitrarily extrapolated up to 90 kip single axle loads, is shown.

The theory that is the basis of the PCA method suggests that rigid pavement failure is the result of fatigue. The repetition of loads can be, for all practical purposes unlimited so long as a flexural stress of 50 percent of the ultimate flexural stress is not exceeded. Each load repetition that causes stress in excess of 50 percent of ultimate contributes to failure. Allowable repetitions at a stress ratio  $f_r/f'_r = 0.51$  is 400,000. At a stress ratio of 0.85, only 30 repetitions could be made. The logarithmic relationship is shown by Figure 23.

Using the design chart of Figure 22, and the allowable load repetitions versus stress ratios of Figure 23, the relative effects of the 85 kip single-axle Euclid load, used for this test, can be compared to an 18 kip single-axle load. A 4-inch pavement on a sub-grade with modulus  $k = 400$  psi/in, the pavement would be stressed to 485 psi; or

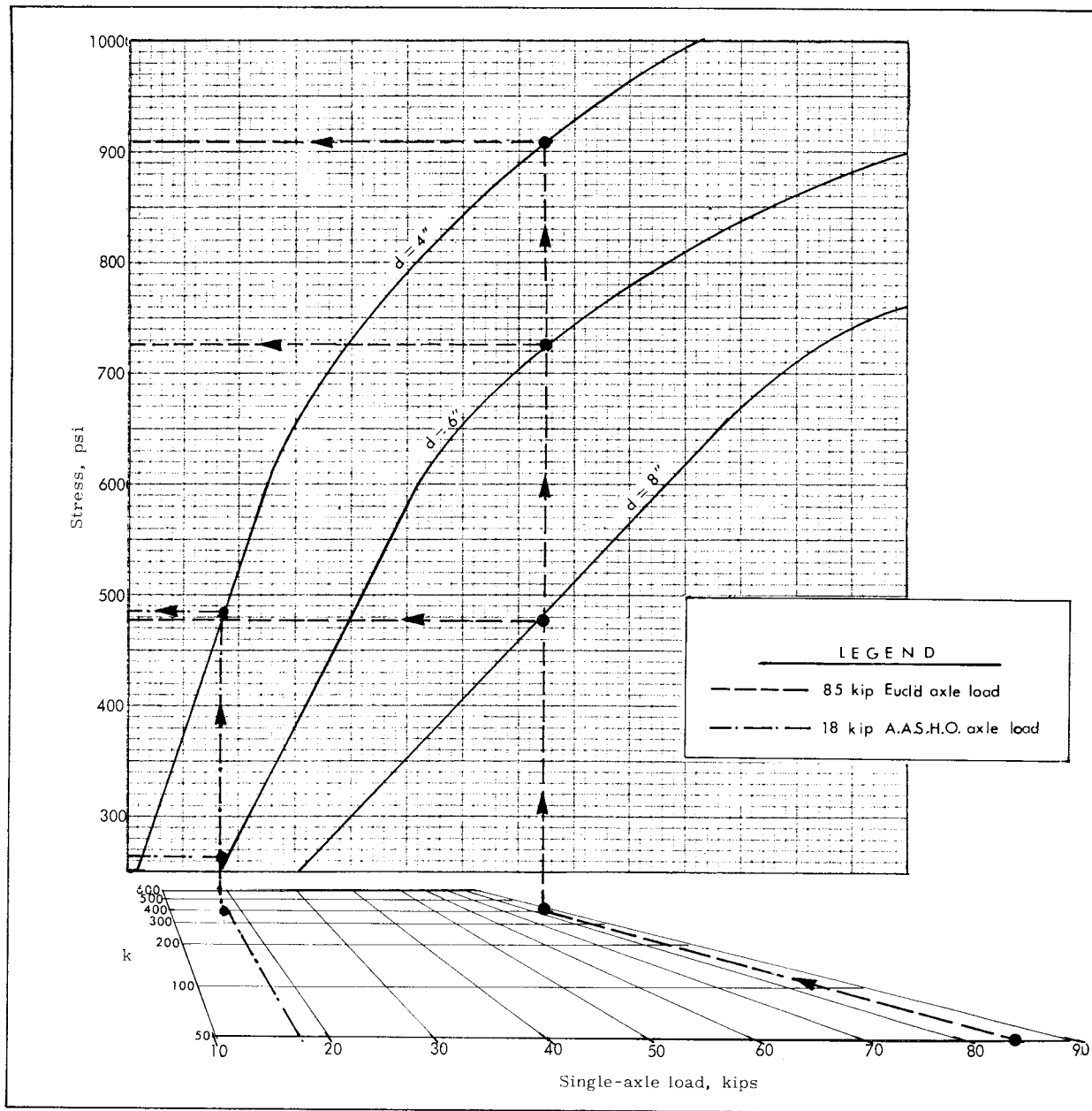


Figure 22: EXTRAPOLATED DESIGN CHART FOR SINGLE-AXLE LOADS AT EDGE OF PAVEMENT

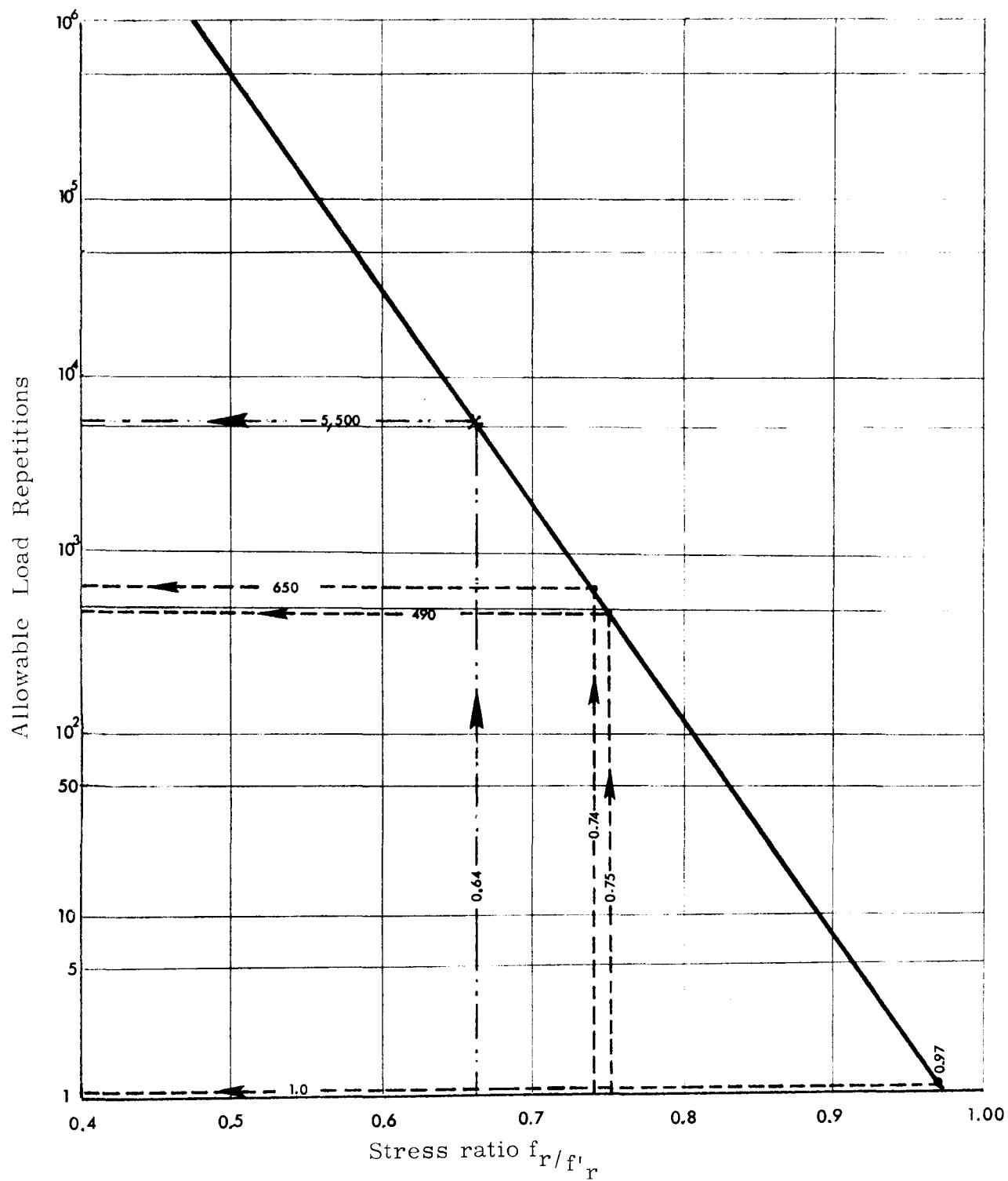


Figure 23: PREDICTED LOAD REPETITIONS ALLOWED FOR VARIOUS STRESS RATIOS (PCA method)

for slab #4, to a stress ratio  $f_r/f'_r = 0.663$ . Allowable load repetitions of about 5500 are indicated by Figure 23. At the same sub-grade modulus of sub-grade reaction, the 4-inch test pavement is stressed in flexure by an 85 kip axle load to 727 psi, a stress ratio of 0.97, and can accommodate but one load repetition. By this approach, then, each of the 85 kip single-axle test loads on the 4-inch slab was the equivalent of 5500 load repetitions by an 18 kip single axle.

An 18 kip single-axle load on a 6-inch pavement induces flexural stress of 265 psi, or a stress ratio for slab #3 of 0.362. The number of repetitions is theoretically, about 3,000,000. Under the 85 kip axle load, slab #3 was stressed to 727 psi, a stress ratio of 0.97, and could accommodate only one or two passes. Each pass is the theoretical equivalent, by this calculation, of the fatigue developed in unlimited applications of normal loadings.

It is realized that the PCA method was not established on the basis of the 18 kip axle load, as the AASHO method is. It also should be pointed out that errors may have been introduced by using the small-scale influence charts. Similarly the extrapolations shown by Figure 22 are admittedly arbitrary and subject, therefore, to error. However, the calculations and comparisons appear to be valid for qualitative assessment. The 85 kip axle loads imposed on the test

pavements provide the means for accelerated testing. Performance results, described in Section 5, can be related and compared to conventional pavements under normal traffic loads.

### 6.3 Conclusions:

The results of this series of service tests of glass fiber reinforced pavements are judged to be significant. It is clearly shown that the randomly distributed fibers enhance performance. Even though the water/cement ratio had been unavoidably increased, decreasing the strength of the concrete matrix, the glass fiber reinforced Slab #2 (8 inches thick) and Slab #3 (6 inches thick) performed better than the conventional steel reinforced Slab #1 as far as "first crack" is concerned.

Attention is invited to Table 6-4, in which the degradation of Present Serviceability Index  $p$  is related to the performance of each slab in terms of equivalent 18 kip single axle load repetitions. The superior performance of the 8 inch glass fiber reinforced Slab #2 is measured with respect to the 8 inch control slab. The relative comparable performance of the 6 inch glass reinforced Slab #3 can be seen also.

In future work, it should be possible to cast a 6-inch pavement

reinforced with glass fibers, and with an ultimate compressive strength,  $f'_c \geq 3000$  psi, that will perform better than the conventional 8 inch steel reinforced pavement. This will require the increase of cement content, up to 8 or 9 bags per cubic yard, in order to provide the cement paste needed because of the increased surface area of the glass fibers that are added to the mix.

TABLE 6-4  
PERFORMANCE SUMMARY

	Slab #1	Slab #2	Slab #3	Slab #4
First crack 18 kip equiv. 18 kip maximum	13 large unlimited	179 very large unlimited	20 $3 \times 10^6$ unlimited	6 5500 $3.3 \times 10^4$
p = 2.5 Equiv. Factor 18 kip equiv.	1028 750.2 $7.75 \times 10^5$	32.2 750.2 $2.42 \times 10^6$	578 884.8 $5.11 \times 10^5$	13 1051 $1.37 \times 10^4$
p = 2.0 Equiv. Factor 18 kip equiv.	3212 911.3 $2.92 \times 10^6$	large 911.3 unlimited	678 961.4 $6.51 \times 10^5$	20 1062 $2.12 \times 10^4$
p = 1.5 Equiv. Factor 18 kip equiv.	large 1070 unlimited	large 1070 unlimited	1028 1070 $1.10 \times 10^6$	116 1070 $1.24 \times 10^5$

The addition of the fibers at the job site proved to be feasible and desirable. Good distribution of fibers was achieved with mix time

of up to 5 minutes. Manual dumping of the pre-chopped glass fibers from their shipping container worked all right; however, the introduction of the fibers into the mixer by the use of an electric or pneumatic chopper could be easier and quicker.

Low slump and poor workability of the glass fiber reinforced batch of fresh concrete requires some additional effort in placement. Vibrators, in adequate number, are essential. Large capacity paving machines, that incorporate vibrators on the front of the travelling screed, would be expected to have no difficulty in placing and compacting the fresh concrete with 1.0 to 1.2 percent glass fibers by volume.

Future pavement trials should be undertaken to optimize concrete batch proportions and placement and finishing techniques. Pavement slabs of 6 inch thickness, properly designed, will probably perform better than conventional 8-inch pavements. The glass reinforced concrete should also be effective for the construction of bridge decks, for pavement overlays, and for repairs by patching of pavements and bridge decks.

The tests reported here have met all test objectives and have provided clear evidence of the potential of glass fiber reinforced pavements or other slab-on-ground structures.